

Microfluidics for particle synthesis from photocrosslinkable materials

David Baah · Tamara Floyd-Smith

Received: 7 September 2013 / Accepted: 4 January 2014 / Published online: 19 January 2014
© Springer-Verlag Berlin Heidelberg 2014

Abstract This paper is a review of microfluidics for particle synthesis from photocrosslinkable materials. Microfluidics for particle synthesis is rapidly gaining attention as a viable method for the synthesis of particles with applications in drug delivery, security, abrasives, rheology, catalysis and other areas. Particle synthesis can follow several schemes, but the focus of this review is particle synthesis from photocrosslinkable materials. In these systems, solid particles are formed by the light-initiated crosslinking of precursor materials. This review begins with a discussion of photocrosslinkable materials, typically synthetic hydrogels for particle synthesis applications. Next, polydimethyl siloxane and glass devices are presented as the primary microfluidic devices for synthesis from photocrosslinkable materials. Then, the review discusses three types of polymeric particles: spherical, spheroidal and Janus. Subsequently, composite particles and metal or metal oxide particles are discussed. The review closes with a discussion of particle throughput and the outlook for the field of particle synthesis from photocrosslinkable materials.

Keywords Microfluidics · Particles · Photocrosslink · Photopolymerize · Lithography

1 Introduction

Microfluidics is a multidisciplinary field intersecting engineering, physics, chemistry, biology and microtechnology with practical applications in the design of systems in which small volumes of fluids are used. Moreover, recent trends in advances could further make the technology more ubiquitous. Potential applications include pharmaceuticals (Cheah et al. 2012; Tao et al. 2011), biotechnology (Liu et al. 2012; Mazzitelli et al. 2011), life sciences (Trietsch et al. 2011), defense (Golden et al. 2012), public health (Mark et al. 2010; Santos-Martinez et al. 2011; Yager et al. 2006), and agriculture (Neethirajan et al. 2011), each of which has its own needs. Hence, the next generation of microfluidics applications emphasizes flexibility and utility in a variety of contexts. One example of a relatively new application is microfluidics for particle synthesis. Microfluidics technology for particle synthesis is considered one of the newest methods of making a library of exotic particles with simple to complex structural characteristics due to its flexibility and potential to create particles of unique chemistries, controllable morphologies and shapes.

In order to understand the value of microfluidics for particle synthesis, one should consider this method in the context of more conventional methods. Whereas conventional methods, such as sol-gel, hydrothermal, crystal growth, suspension (Yamagami et al. 2013) and microemulsion polymerizations (Gokmen and Du Prez 2012), are suitable for the synthesis of spherical particles, the application of these protocols to the synthesis of non-spherical particles is limited due to the surface energy compatibility of the particles. Consider, for example, the case of microemulsion polymerization. Lu et al. (2007) described microemulsion polymerization as the polymerization of a

D. Baah · T. Floyd-Smith (✉)
Materials Science and Engineering Department, Tuskegee University, 522A Foster Hall, Tuskegee, AL 36088, USA
e-mail: tfloyd@mytu.tuskegee.edu

T. Floyd-Smith
Chemical Engineering Department, Tuskegee University,
Tuskegee, AL 36088, USA

thermodynamically stable isotropic dispersion of two immiscible liquids in which the micro-domain, being the continuous or dispersed phase, is stabilized with surfactant molecules. In water-in-oil microemulsions, the aqueous phase consists of micro-droplets surrounded by surfactant molecules in a monolayer. The micro-droplets are polymerized by addition of appropriate solvents. Precise control of the particle size and dispersity is largely dependent on reactor conditions and can be difficult to control. Moreover, particle shape is limited to spherical. Next, consider the case of solution-based synthesis of inorganic or metallic particles. The precise control and tuning of particle size and shape in such solution-based synthesis, which is dictated by nucleation and growth, is determined by thermodynamics factors (e.g., temperature, and reduction potential) and kinetics factors (e.g., solubility, reactant concentration, diffusivity, and the rate of reaction) (Tao et al. 2008). Managing the interplay of these factors with particle size and shape control is almost serendipitous once the correct synthesis chemistry and additives are identified to manipulate crystallographic planes. However, a more general platform would increase the rate at which new particles can be synthesized and tested as potential applications become apparent.

Microfluidics flow-based lithographic technology for particle synthesis is bridging the gap between platform generality and control of particle shape, size, morphology, and other structural characteristics and features. A closely related lithographic-based method for synthesizing particles with predetermined structural features is DeSimone's Particle Replication in Non-wetting Templates (PRINT[®]) technique (Gratton et al. 2007, 2008; Rolland et al. 2005). In the PRINT method, a mold, coated in a low surface energy perfluoropolyether (PFPE)-based elastomer and patterned with motifs defining the particle shape, is filled with a precursor solution (Rolland et al. 2005). Particles are formed either by (1) exposure of the precursor in the mold to UV light which triggers photoreaction to form the particles or (2) exposure to elevated temperatures in an oven which trigger particle formation by other means such as a sol-gel reaction. Without regard to the method of particle formation, the particles are created in the size and cross-sectional shapes of the motifs from which they are formed. Using this approach, it is possible to synthesize particles with sizes down to the nanometer size range with different composition, structural features, and mechanical properties (Merkel et al. 2010, 2012; Nunes et al. 2010). However, a challenge of the PRINT approach to synthesizing non-spherical particles is the bending and buckling of the template which may limit the transfer of patterns with high-aspect ratio (Helgeson et al. 2011). Furthermore, releasing the particles through template dissolution and scalability is

another source of concern with the PRINT method (Merkel et al. 2010).

Microfluidics technology, however, provides a versatile platform to design, model, synthesize and control particle properties (Cederquist et al. 2010; Chung et al. 2011; Luo et al. 2011; Tan et al. 2012) that is a competitive alternative to the PRINT method. Using the microfluidics platform provides an alternative route for the synthesis of a plethora of functional materials such as polymeric particles and their hybrids or composites, microfiber, colloidosome, Janus particles, and anisotropic particles because it offers the flexibility to precisely control particle shape, size, chemical compartmentalization, and core/shell structures. Recent reviews of the literature on this subject focused on discussing the synthesis of organic and inorganic micro- and nanostructures and their composites (Marre and Jensen 2010; Park et al. 2010), and the synthesis and assembly of polymeric microparticles using lithographic processes (Dendukuri and Doyle 2009; Helgeson et al. 2011). Additionally, microfluidics approaches to cell encapsulation in hydrogel particles and the applications for drug delivery in cancer therapy have been discussed by Wan (2012). Most recently, Kim et al. (2013) and Shim et al. (2013) provided detailed reviews discussing design strategies for producing functional microparticles and controlled encapsulation and release studies using droplet microfluidics techniques, respectively.

In this review, recent advances in the application of microfluidics for particle synthesis from photocrosslinkable materials are discussed. The objective of this review is to highlight the unique potential of microfluidics technology to synthesize micron to nanoscale particles of unique structural features from photocrosslinkable precursors and discuss very recent advances as well as future prospects of particle morphological design for specific applications. First, the paper discusses photocrosslinkable hydrogel precursors as the material of choice for particle synthesis from photocrosslinkable materials. These are a class of polymers compatible with microfluidics technology due to their UV transparency, water solubility, and suitable free radical polymerization reaction kinetics. Next, the types of microfluidics devices that enable particle synthesis from photocrosslinkable materials are described. Then, the synthesis of spherical, spheroidal and two-dimensionally extruded homogeneous polymeric particles is discussed. Janus particles, which are multiphase particles demonstrated as both spherical and two-dimensionally extruded, are discussed separately. Next, the discussion expands to composite and inorganic particles. Finally, particle throughput is discussed, and suggestions for future research related to investigating other synthesis materials, particle size reduction, and applications are discussed.

2 Photocrosslinkable materials: focus on hydrogels

Hydrogels are a cross-linked or three-dimensional network of polymer chains that are hydrophilic and sometimes found as a colloidal gel in which water is the dispersion medium. They are highly absorbent and can absorb 10–20 times their molecular weight when swollen in water (Singh et al. 2010). Specifically, however, this review discussion is limited to the use of photocrosslinkable hydrogels because of their fast reaction kinetics (Burdick et al. 2001; Dendukuri et al. 2008), water solubility, chemical compatibility with polydimethylsiloxane (PDMS) microfluidic devices and suitability as a host for inorganic nanoparticles. The inorganic particles are introduced to tailor hydrogel properties (Alveroglu et al. 2013; Shepherd et al. 2006) and also provide an indirect route to the synthesis of non-spherical inorganic particles (Baah et al. 2013; Shepherd et al. 2008).

2.1 Hydrogels in microfluidics

Hydrogel polymers are broadly characterized into two groups: (1) hydrogels obtained from natural sources and (2) synthetic hydrogels obtained by polymerization reactions. Ifkovits and Burdick (2007) and Wan (2012) compiled a comprehensive list of natural and synthetic hydrogels summarizing their precursors and gelation mechanisms, cross-linking methods, as well as their advantages and disadvantages for cell encapsulation. Such data provide information for selecting hydrogel precursors knowing the mode and kinetics of cross-linking, cell compatibility, hydrophobicity, and mechanical strength of the hydrogel. A characteristic feature of hydrogels is their provision of a protective environment for drugs and proteins from particularly harsh environments in the area surrounding release (Langer and Peppas 2003). As a result, hydrogels are increasingly being developed as carriers for bioactive and bioadhesive agents. While synthetic hydrogels are largely inherently bio-inactive polymers, there is a growing interest in their use in microfluidics applications for particle synthesis. Beebe et al. (2000) are, to the authors' knowledge, the first to demonstrate microfluidics for particle synthesis to synthesize micron-scale hydrogel particles usable as micro-actuators. Subsequently, poly(ethylene glycol) (PEG) hydrogel microstructures, attached to a surface and on the order of 10 μm , were fabricated in microfluidics devices for potential use as biosensors and for cell adhesion (Koh and Pishko 2003). Further, Burdick et al. (2004) demonstrated the fabrication of hydrogel thin films with gradients in (1) adhesive ligands that modulated the spatial distribution of attached endothelial cells and (2) cross-linked densities with variable water swelling potentials. This spatial control over cross-link densities allows the development of injectable materials that can deliver

cells and growth factors and, also, the fabrication of scaffolding materials with complex microstructures. In another application, the fabrication of gradient poly(ethylene glycol) diacrylate (PEG-DA) thin films with dispersed fluorescent polystyrene nanoparticles or high refractive index TiO_2 nanoparticles was demonstrated using microfluidics devices (Baah et al. 2008, 2011). These studies, though targeted toward the fabrication of gradient materials for optical applications, contributed to further stimulate the idea of incorporating inorganic nanoparticles into photocrosslinkable precursors for the purpose of making composite particles.

2.2 Free radical polymerization reaction of hydrogels

Photo-initiated free radical polymerization reactions are important for obtaining a wide variety of polymers and material composites. The relatively non-specific nature of free radical polymerization interactions makes it one of the most versatile forms of polymerization reactions available and allows facile reactions of polymeric free radical chain ends. Most importantly for microfluidics synthesis of particles, for example, using mono- or diacrylated poly(ethylene glycol) in the presence of a suitable photo initiator, the rate of the free radical polymerization reaction is on the order of milliseconds. The fast reaction time is critical toward enabling rapid bulk synthesis of particles. The rate of reaction initiation is dependent on parameters such as the initiator efficiency, initiator concentration, and light intensity. During polymerization, the free radicals propagate through unreacted acrylic double bonds to form long kinetic chains. The reaction initiation rate is expressed in the equation

$$R_i = 2\Phi f I, \quad (2.1)$$

where Φ is the quantum yield, f is the photo initiator efficiency, and I is the light intensity. However, the overall rate of consumption of double bonds is given by Eq. 2.2 (Burdick et al. 2001; Cowie and Arrighi 2008).

$$-\frac{d[M]}{dt} = k_p[M] \left(\frac{R_i}{2k_t} \right)^{\frac{1}{2}} \quad (2.2)$$

In Eq. 2.2, $[M]$ represents the concentration of double bonds in the precursor, k_p is the propagation kinetic constant, k_t is the termination kinetic constant and t is the time of polymerization. Once the reaction is initiated, free radicals propagate through unreacted double bonds to increase the kinetic chain. The rate constants change with both monomer conversion and temperature in diffusion-controlled reactions. Free radical polymerization is an exothermic process, and, as the polymerization progresses, the temperature of the reaction medium rises. It follows from Eq. 2.2 that higher initiator concentration increases the

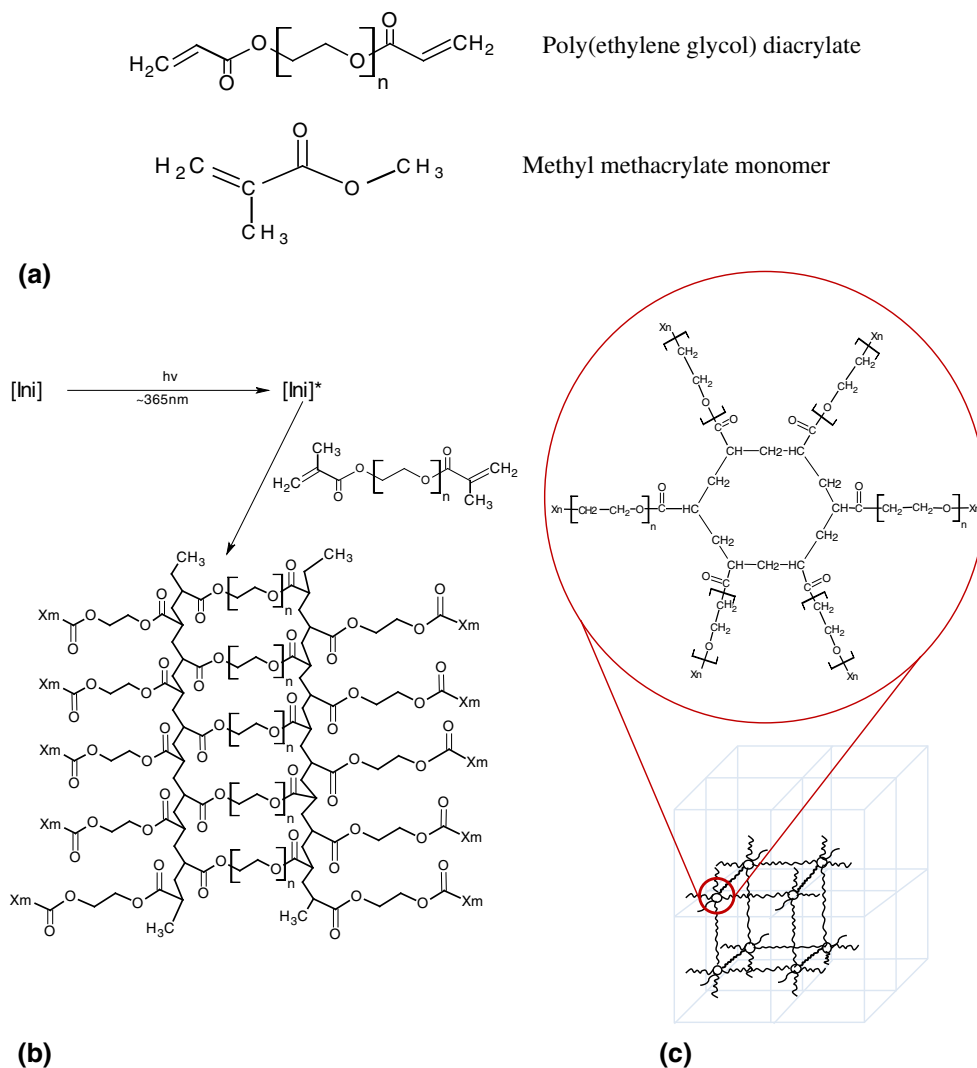


Fig. 1 **a** Representative structures of poly(ethylene glycol) diacrylate pre-polymer and methyl methacrylate monomer commonly used as precursors in microfluidics for particle synthesis. **b** Schematic photo polymerization reaction of the poly(ethylene glycol) pre-polymer

reaction rate. As the temperature increases, the rate of polymerization also increases with a further increase in the amount of heat generated (Burdick et al. 2001; Fouassier et al. 2003; Ifkovits and Burdick 2007; Nguyen and West 2002). However, the exothermic heat produced ($Q \propto -d[M]/dt$) is detrimental to the lifespan of the microfluidics devices during particle synthesis. Figure 1a shows a simple structural representation of PEG-DA and methyl methacrylate monomers (or pre-polymers), and Fig. 1b is a representation of the cross-linked PEG-DA based on the studies of the network structure of UV-cured acrylates using ^1H NMR, ^{13}C NMR, and DMA experiments (Litvinov and Dias 2001). According to Litvinov and Dias (2001), the nature of the cross-linked network affects not only the macroscopic properties (e.g., mechanical properties), but also microscopic properties such as the diffusion

showing the network structure of the cross-linked polymer. **c** Theoretical elucidation of the cross-linked network depicting simple cubic unit cell with cyclododecane vertices

of small molecules such as nutrients for cell viability in living biological systems, active biomolecules, and other solutes. A physical model proposed by Wu et al. (2009) suggested that for methyl methacrylate monomer or PEG-DA pre-polymer (Fig. 1a), an idealized basic structural unit consists of a simple cubic unit cell with cyclododecane rings at the vertices (Fig. 1c). Using different cross-linking densities (defined as the reciprocal of the degree of polymerization of the PEG chain, $1/n$), the study found that the diffusion coefficient of water and other small molecules decreases with increasing cross-linking density. In Table 1 (Wu et al. 2009), a summary of the system composition and mesh size as well as other properties of the simulated system is shown. However, structural heterogeneities with respect to the cross-linking density, mesh size, and percent polymer content exist in the cross-linked network due to

Table 1 System composition and equilibrated mesh size for varying molecular weight of PEG. The Table is adapted with permission from Wu et al. (2009). © American Chemical Society

Pre-polymer	PEG572	PEG1000	PEG1500	PEG2000	PEG3400
<i>N</i>	13	23	34	45	78
Cross-linking density (1/ <i>n</i>) %	7.69	4.35	2.94	2.22	1.28
Equilibrated water content/%	74.7	84.2	85.5	89.9	90.0
Polymer volume content/%	25.3	15.8	14.5	10.1	9.1
Mesh size/nm	2.28	3.14	3.64	4.47	5.49
Number of water molecules/cell	291	855	1,353	2,636	4,984
Number of cells	2 × 2 × 2	2 × 2 × 2	2 × 2 × 2	1 × 1 × 1	1 × 1 × 1
Simulation box size/nm	4.56	6.28	7.28	4.47	5.49

n is the degree of polymerization before cross-linking

the nature and composition of the pre-polymer solution determined by the concentrations of the precursor and initiator as well as light attenuation.

3 Microfluidics devices

The flow of a fluid through microchannels is characterized by the Reynolds (Re) number, arising from the non-dimensionalization of the Navier–Stokes equation. The Reynolds number is defined as

$$Re = \frac{Lv_{avg}\rho}{\mu} \quad (3.1)$$

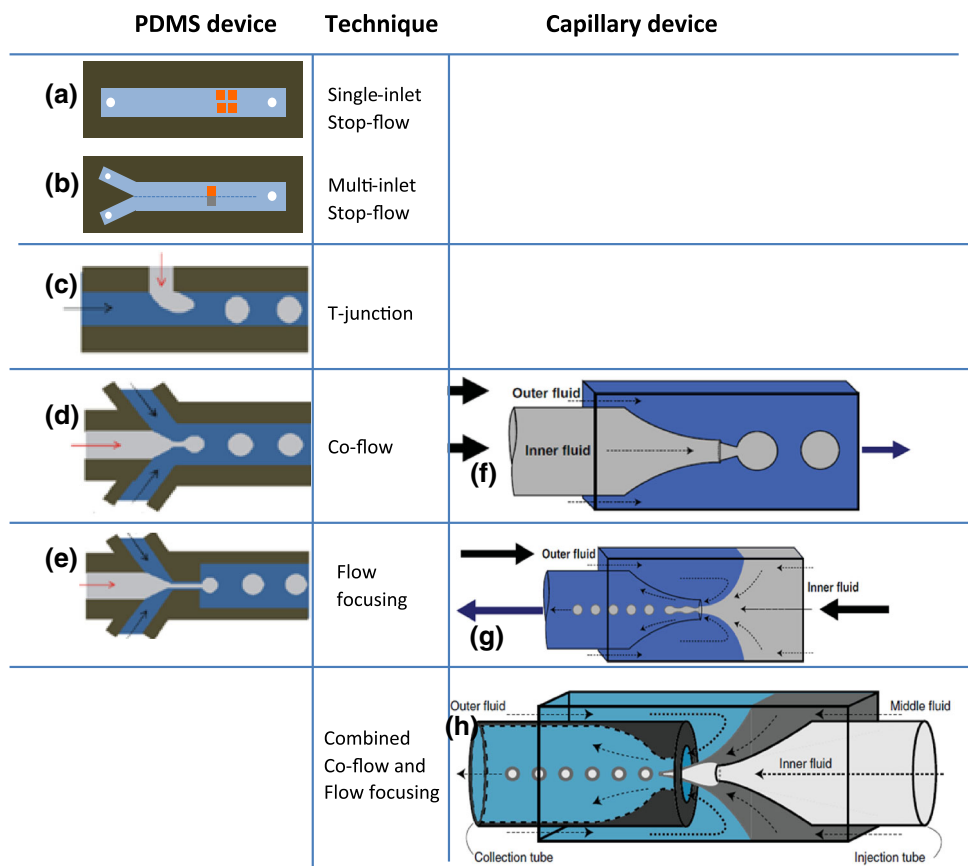
where L is the most relevant length scale, μ is the fluid viscosity, ρ is the fluid density, and v_{avg} is the average velocity of the fluid (Kumacheva and Garstecki 2011). For many microchannels, L is equal to $4A/P$ where A is the cross-sectional area of the channel and P is the wetted perimeter of the channel. Due to the small dimensions of microchannels, the Re is much less than 100, often less than 0.1. In this Reynolds number regime, the flow is completely laminar and no turbulence occurs. Laminar flow provides a means by which molecules can be transported in a relatively predictable manner through the microchannels. The laminar flow of fluids in small capillaries permits multiple streams of solutions containing different concentrations to flow side-by-side without turbulence. This fluid dynamic phenomenon is particularly important for the distribution of solution species during synthesis using single or multiphase solution streams in microfluidic devices. In the past, review articles have been published in which the applications of these devices in particle synthesis are discussed (Dendukuri and Doyle 2009; Gokmen and Du Prez 2012; Helgeson et al. 2011; Marre and Jensen 2010; Park et al. 2010).

Microfluidics devices are classified into two major groups, the first being PDMS based devices originated by the Whitesides' Research Group (McDonald and Whitesides

2002; Qin et al. 2010; Weng et al. 1999; Xia et al. 1999). The PDMS elastomer possesses unique properties that make it suitable for the fabrication of microfluidics devices. The elastic nature allows conformal contact with glass slides and non-planar substrates. Irreversible bonding to glass slides is facilitated by an oxygen plasma treatment which renders the surface of the PDMS stamp hydrophilic and reactive such that it can form irreversible bonds with a glass substrate. The PDMS based devices are found to be less expensive, reusable, and straightforward to fabricate (McDonald and Whitesides 2002). A unique advantage of the PDMS device is the compatibility with aqueous solvents and its transparency to UV light. However, the swelling of PDMS in non-polar solvents is a drawback hindering its generality of applications. Lee et al. (2003) provide a useful guide for solvent selectivity based on solubility parameters. It is also worthwhile to note that there have been efforts to functionalize the PDMS surface to improve its solvent compatibility (Abate et al. 2008). The second class of microfluidic devices currently in use is glass systems. The Weitz Research Group (Utada et al. 2007) is credited as the originators of the initial design and fabrication of glass-based microfluidics devices. A drawback with the glass-based devices is the high expertise required for their fabrication as well as the lack of applicability to synthesizing two-dimensionally extruded particles.

Figure 2 depicts a broad characterization of the specific types of microfluidic devices that are currently in use for both PDMS and glass. The PDMS devices, which are relatively easy to fabricate and also construct into different forms, are generally used to make spherical particles, multi-phase particles (Janus particles), and two-dimensionally extruded non-spherical particles whose cross-sectional shapes can be varied. Glass capillaries are also used to make spherical and multi-phase particles. Modifications of flow parameters and solvent combinations can be used to make particles with unique structures. For example, Fig. 3a–d demonstrates the utility of microfluidics to synthesize two-dimensionally extruded particles with different

Fig. 2 Schematics of representative microfluidic devices currently in use: *a* single, *b* multi-inlet, *c* t-junction, *d* co-flow and *e* flow-focusing devices fabricated in PDMS; *f* co-flow, *g* t-junction and *h* flow-focusing devices fabricated in glass. *c–e* from Gokmen and Du Prez (2012) with permission. © 2011 Elsevier Ltd. *f–h* from Utada et al. (2007) with permission. © 2007 Materials Research Society



cross-sectional shapes using a single inlet PDMS device (Baah et al. 2012; Diao et al. 2011). A homogenous precursor stream is exposed to patterned UV light to create particles in a semi batch process. The microchannel confines the particle axial dimension and creates a horizontal plane of the fluid in which to pattern the particle cross-section. Similarly, Fig. 3e shows the use of a multi-inlet device to create particles of distinct structural anisotropy labeled F1, F2 and F3 (Bong et al. 2010). Laminar flow allows miscible streams to flow side-by-side with minimal mixing in order to create anisotropic particles. Finally, Fig. 3f is a demonstration of the use of a flow-focus device to produce highly monodisperse poly (ethylene glycol) microspheres in continuous droplet formation and in situ photopolymerization. The authors investigated the flow patterns for which stable droplets form at optimum flow rates using hexadecane as the continuous phase. The resulting microspheres showed narrow size distribution in the range of $\sim 45\text{--}95\ \mu\text{m}$ (Choi et al. 2009).

4 Spherical polymeric particles

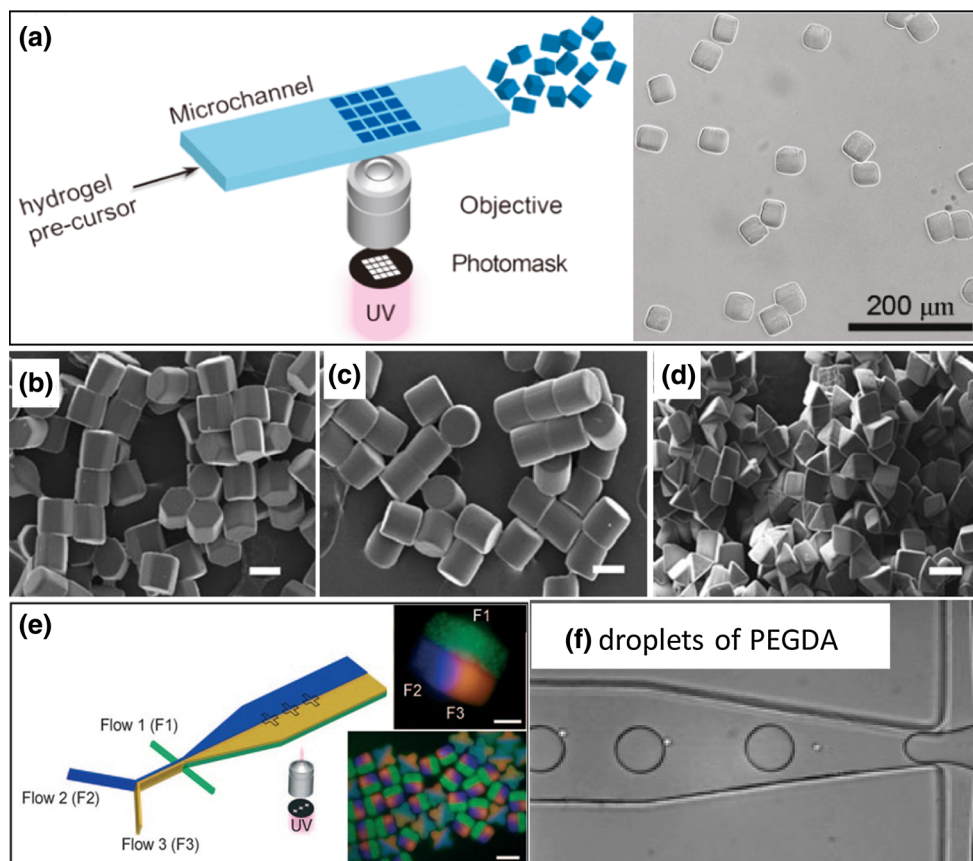
Microfluidics as a tool for the synthesis of spherical polymeric particles and their composites/hybrids is dependent on (1) the formation of fluid droplets of the precursor and (2)

the transformation of this droplet into a gel particle usually through photopolymerization. Thus, a liquid droplet is the precursor to the particle formed and the physical and chemical characteristics of the droplet are transferred to or mimicked in the gel particle. In the words of Gokmen and Du Prez (2012), “an ultimate control over droplet formation is achieved by the youngest particle production technique called Microfluidics.” Droplet formation is achieved using T-junction, Flow-focus, Co-flow and combined Co-flow and Flow-focusing devices shown in Fig. 2. The droplets, which consist of the precursor reagent, are dispensed on demand (one-by-one), into a continuous stream of flowing surfactant. The detailed mechanics of droplet formation is beyond the scope of this review; however, the rudiments are discussed. The basis of emulsification of one fluid (oil) in another (water) is the interfacial tension whose minimization favors the formation of a spherical shape. At the microscale, the influence of gravitational forces is neglected, and the droplet formation and breakup in the flow are controlled in part by the Weber number (We) which characterizes the interface between two liquids and is expressed as

$$We = \frac{\rho Lv^2}{\sigma} \quad (4.1)$$

where ρ is the mass density, σ is the interfacial tension, L is a characteristic length scale, and v is the velocity. The

Fig. 3 **a** Representative single inlet device for making two-dimensionally extruded particles by exposure of precursor solution to patterned UV light. The figure is adapted from Diao et al. (2011). © 2011 American Chemical Society. **b–d** represent a collection of two-dimensionally extruded particles in hexagonal, circular, and triangular cross-sectional shapes formed in a single inlet device. Image is adapted from Baah et al. (2012). © The Authors 2011. **e** Representative multi-inlet device for making two-dimensionally extruded particles with structural anisotropy. The features of the particles are distinguished in colors in the fluorescent micrographs and labeled F1, F2, and F3. The image is adapted with permission from Bong et al. (2010). © 2010 Wiley–VCH Verlag GmbH & KGaA. **f** Representative flow-focus device (color figure online)



Reynolds (Re) which expresses the relative importance of inertial and viscous forces is given in Eq. 3.1. However, in microchannels, the flow regimes are predominantly laminar for which both We and Re are low (usually less than 1) and the possibility of species mixing is only by diffusion. A more important dimensionless parameter, capillary number (Ca), which expresses the relative effect of viscous forces and surface tension, represents a combination of We and Re . The capillary number is given by

$$Ca = \frac{\mu v}{\sigma} \quad (4.2)$$

and expresses the competition between interfacial stresses and viscous stresses. For example, in the absence of interfacial tension between two immiscible liquids, the two streams would flow side-by-side after meeting at a T-Junction. However, in reality, the competing stresses control the interface with surface tension acting to reduce the interfacial area while the viscous stresses act to extend and drag the interface downstream. The combined stresses destabilize the interface and cause droplets to form. The diameter of the droplets is directly related to the dimensions of the channels from which they are formed (Chung et al. 2011; Gu et al. 2011; Rotem et al. 2012; Xuan et al.

2010; Zeng et al. 2011). Abate and Weitz (2011) described the drop formation physics as a “plugging/squeezing mechanism” in which the drop size depends on the flow rate ratio of the dispersed-to-continuous phase. Figure 4a–c shows pictures of droplets formed in the T-junction, Flow-focus, and Co-flow devices, respectively. The images show that the particle size, which is dependent on the droplet size, is related to the channel dimensions. The droplet in Fig. 4a is stretched and on photocrosslinking will produce particles that are oblong-shaped, whereas the droplets in Fig. 4b, c will form perfectly spherical particles. In Fig. 5d, highly monodisperse spherical particles of poly(methyl methacrylate) (PMMA) are formed as a result of photocuring droplets formed at the flow-focus junction in a device illustrated schematically in Fig. 5a, b. Further, Fig. 5c shows the stream of precursor droplets en route to the region of exposure for cross-linking. The average particle size is $\sim 10 \mu\text{m}$. Lin et al. (2012) developed a new, on-demand droplet generator for selective fluid sample extraction. In this work, the channel design (Fig. 6a) allows a droplet to split under quasi-steady-state conditions, thereby reducing the ultimate particle size as well as controlling the amount of species to be encapsulated. In Fig. 6a, the blue lines indicate the dispersed phase channel, the yellow line represents the continuous phase channel,

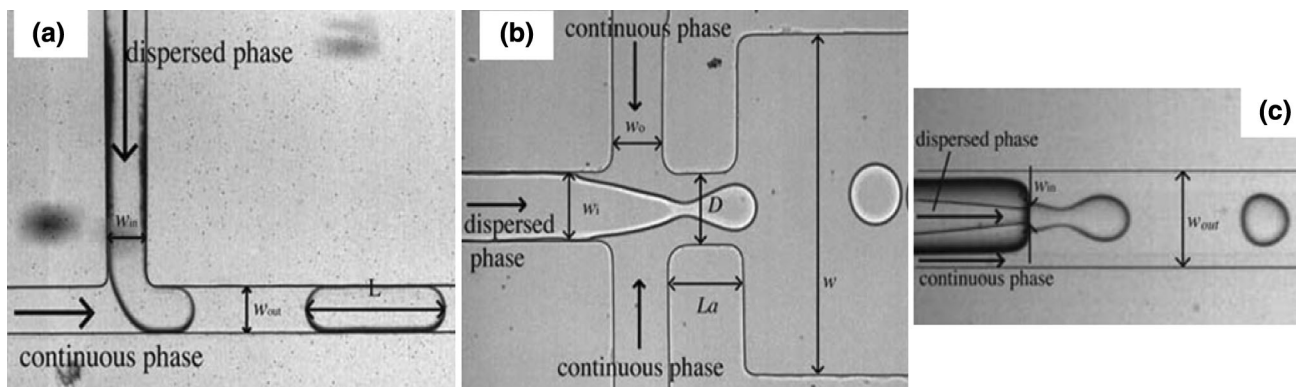


Fig. 4 Micrographs showing droplet formation in **a** T-Junction, **b** Flow-focus and **c** Co-flow devices. The images are adapted with permission from Baroud et al. (2010). © 2010 The Royal Society of Chemistry

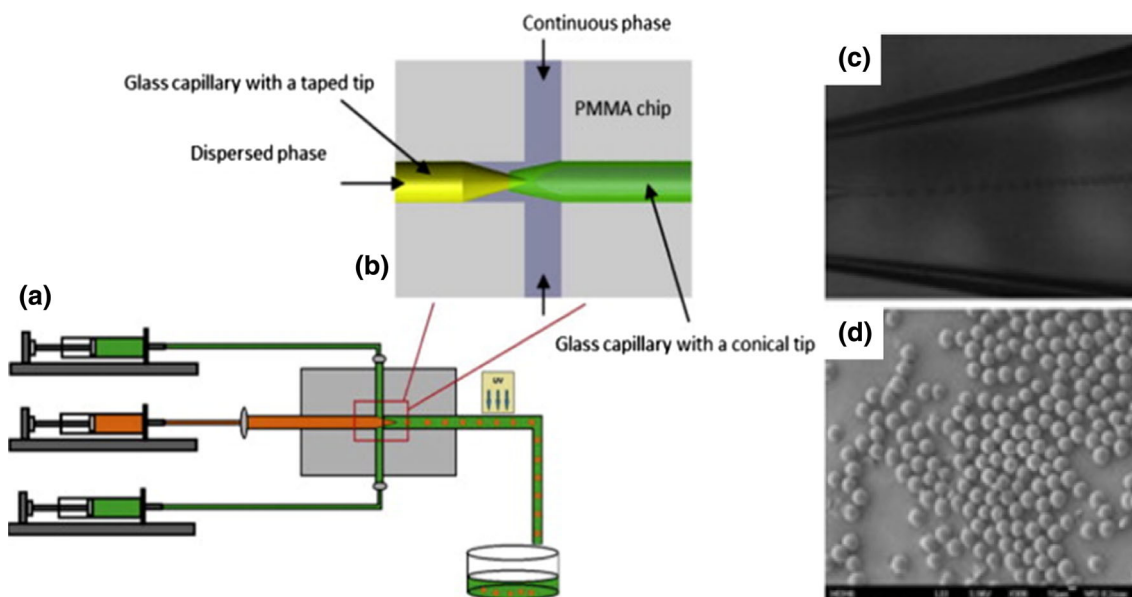


Fig. 5 **a** Flow-focusing schematic, **b** enlargement of the droplet formation area **c** micrograph of a stream of particles en route to the exit/collection area. **d** SEM micrograph showing highly monodisperse

particles of $\sim 10 \mu\text{m}$ diameter. The images are used with the permission of Dong et al. (2013). © 2013 Elsevier Ltd

and the green line is the control channel. The red square represents the droplet generation region of the device. The inset (Fig. 6b) provides a clearer description. The blue arrow in the inset (Fig. 6b) shows the direction of the dispersed phase flow. The red arrow denotes the ground outlet flow direction. The yellow arrow indicates the flow direction of the continuous phase and the flow direction of the generated droplet. Figure 6c is a picture of what is schematically represented in Fig. 6b. In Fig. 6d, the red lines indicate the paths of three beads that were not encapsulated into the formed droplet while the green lines represent the paths of beads that were encapsulated when a droplet is generated. The starting location of the beads is marked with open circles. The total time taken for a single drop to develop and break-off from the droplet junction is approximately 48 ms. The potential of microfluidics for

producing particles of high monodispersity is limitless as long as a system of miscible nonpolar organic solvents can be emulsified in an aqueous phase, and vice versa (Kuehne and Weitz 2011).

One strength of microfluidics for synthesizing particles is the potential to precisely control properties including dimension, shape, morphology, composition, and structural anisotropy. For example, droplet formation in microfluidics has been applied to the production of designer particles (Duncanson et al. 2012; Pawar and Kretzschmar 2010; Shah et al. 2008; Wang et al. 2010). Designer particles are particles of specific complexities and properties designed for a unique function. Using the microcapillary platform in different configurations, it is possible to develop particles for biotechnology applications in chemical sensing, cell encapsulation, and target drug delivery agents (Giridharan

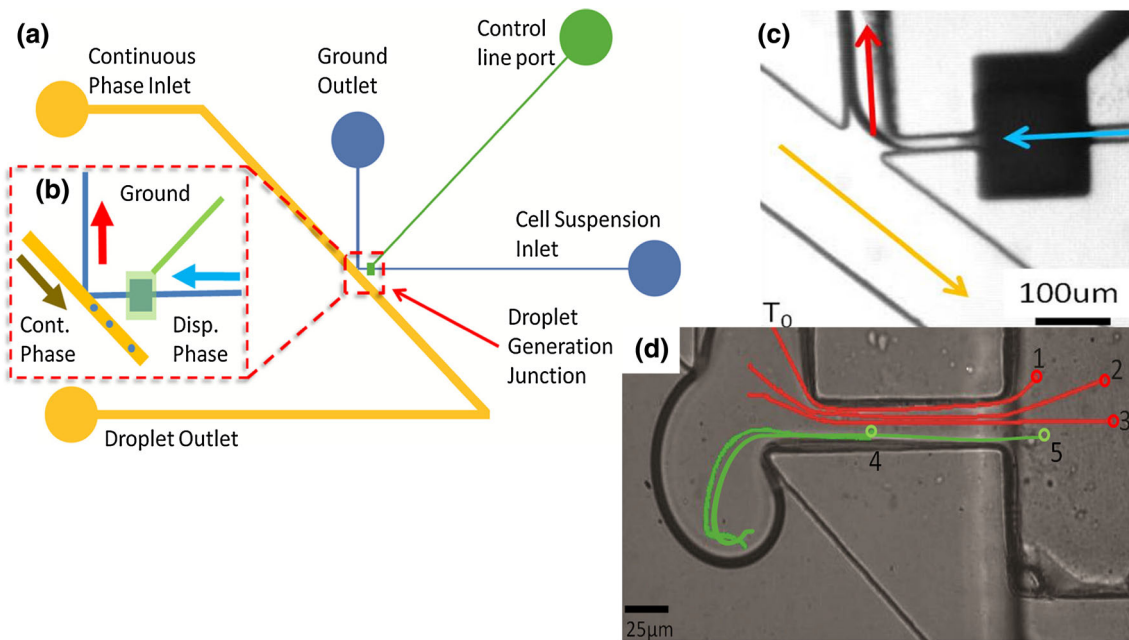


Fig. 6 **a** Schematic of an on-demand droplet generation device. *Inset* **b** The droplet generation area enlarged. **c** optical micrograph of the droplet formation area. **d** optical micrograph showing the extent of

maximum deformation of the dispersed phase into the main fluidic channel. The image is adapted with permission of Lin et al. (2012). © 2012 American Institute of Physics

et al. 2012; Kantak et al. 2012; Zhang et al. 2012) as well as smart microgels (Motornov et al. 2010; Seiffert and Weitz 2010; Seiffert et al. 2010). For example, in one application of particles synthesized using microfluidics, the release profile of encapsulated substances was been shown to correlate with the particle structure and composition (Wassen et al. 2012). Figure 7a–d shows schematics of the use of capillary devices to design particles from droplets using a flow-focusing capillary device. To generate droplets in flow-focusing configuration, the continuous phase is injected through an outside channel and the dispersed phase is injected through a central channel into a narrow orifice to create a strong extensional flow. One liquid flows into two inlet channels surrounding a center channel containing a second immiscible liquid. The two liquids are forced to flow through a small orifice downstream. Pressure and viscous stresses from the outer fluid force the inner fluid into a narrow thread, which breaks downstream of the orifice. The geometry of the junction and the flow rates as well as the physical properties (interfacial tension and viscosity) of both the dispersed phase and continuous phase determine the local flow field and the eventual droplet break-off (Abate et al. 2010; Serra and Chang 2008). Figure 7e is a collection of optical micrographs showing droplet(s)-in-droplet as precursors for designer particles. The technique is used by Lee et al. (2012) to demonstrate the generation of near-infrared (NIR)-sensitive poly(lactico-glycolic acid) (PLGA) microcapsules with programmable release properties achieved by controlling the

morphology of the microcapsules. The PLGA microcapsules are designed as double emulsion droplets based on water-in-oil-in-water (W/O/W). The inner phase (W) is phosphate buffered saline (PBS), and the outer phase (W) is aqueous 2 % poly(vinyl alcohol) (PVA). The middle (O) phase consists of PLGA in a mixture of volatile organic solvents, toluene, and chloroform. Further, gold nanorods (AuNR) were added to the PLGA phase and the emulsion consolidated into PLGA/AuNR nanocomposite microcapsules. Figure 8 shows results for the release of encapsulated fluorescein-isothiocyanate (FITC)-dextran material from PGLA/AuNR capsules in response to external stimuli. The release experiments are performed within 3 days of capsule preparation. It is observed from the significant decrease in fluorescent intensity that the PLGA/AuNR nanocomposite capsules deformed and released the encapsulated FITC-dextran on near-infrared (NIR) exposure. In this case, NIR light is used as the external stimulus because it is minimally absorbed by body water and hemoglobin and readily penetrates the skin. Additionally, it is relatively simple to localize the application of NIR light in vivo compared with other stimuli such as heat and pH. In Fig. 8a, the application of NIR light to neat PLGA microcapsules formed using PLGA 50:50 in pure chloroform does not induce any changes in the shape and the fluorescence intensity. This demonstrates the insensitivity of PLGA capsules to NIR light. However, the AuNR/PLGA nanocomposite microcapsules with a homogeneous shell deformed and released encapsulated FITC-dextran after

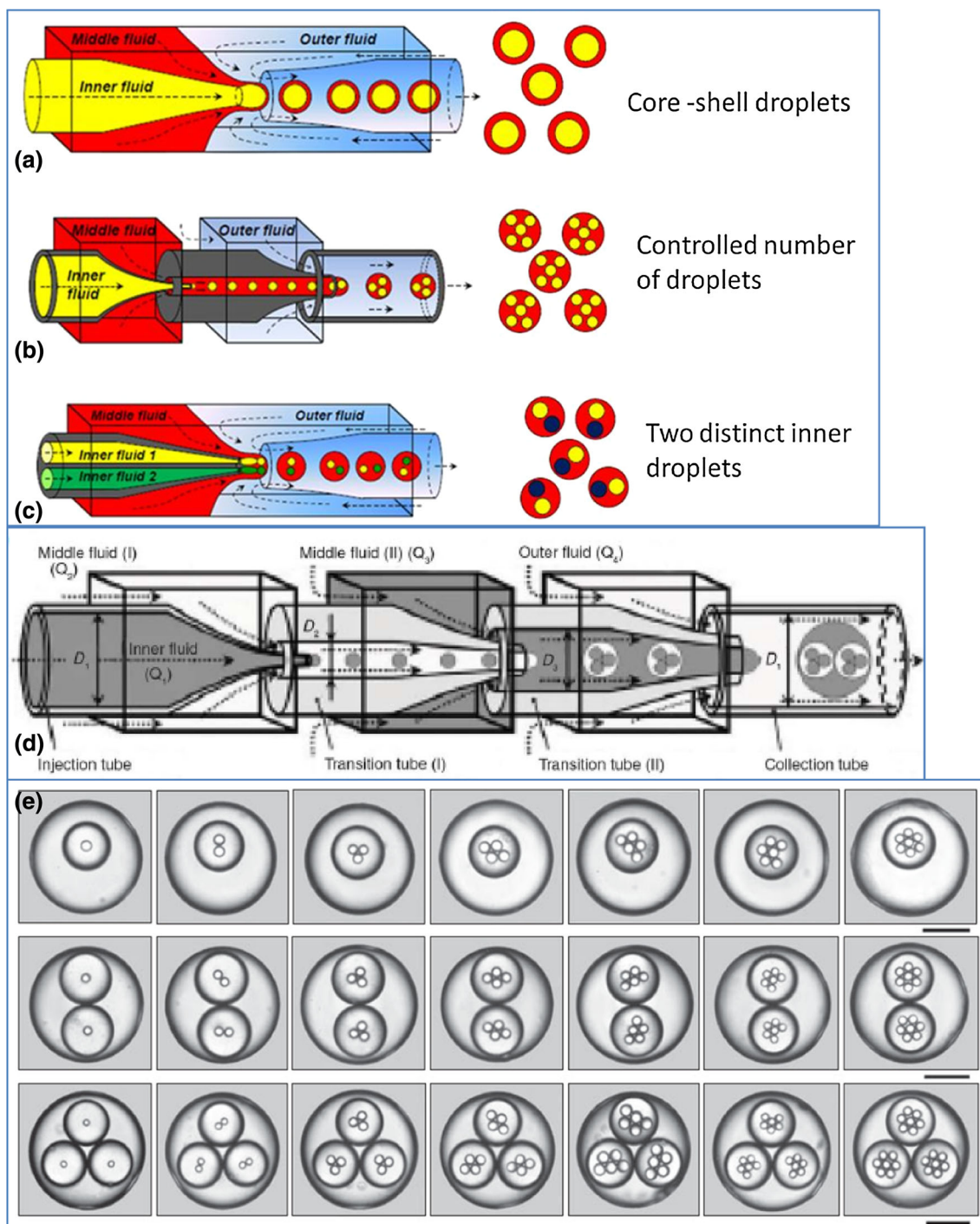


Fig. 7 Capillary devices in different configurations and the artist's rendition of potential particles that can be made in each device: **a** core-shell particles, **b** multi-droplet core-shell particles, **c** multi-dissimilar droplet core-shell particles and **d** multi-core droplets.

e monodisperse triple emulsions made with cascaded microcapillary device. Both the number and size of each of the sets of inner drops can be precisely controlled. *Scale bars* are 200 μm . **d–e** are adapted from with permission from Shah et al. (2008). © 2008 Elsevier Ltd

NIR light exposure (Fig. 8b). Further, the fluorescence intensity profiles of NIR light irradiated samples show that NIR induces essentially the complete release of the encapsulated FITC-dextran, whereas little release is detected from PLGA microcapsules without AuNR

(Fig. 8c, d). Kim et al. (2009) also adapted the approach of droplet generation in microfluidics devices to fabricate submicron particles with complex surface functionalities using a photocurable droplet precursor. Glass capillary devices in coaxial arrangement enabled the generation of

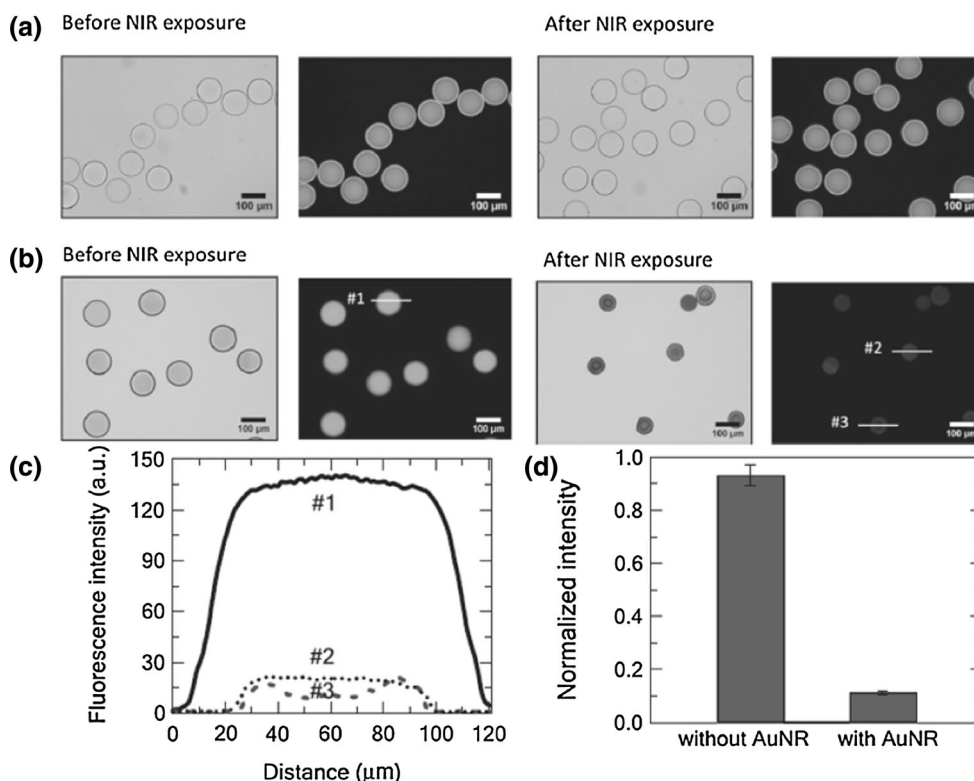


Fig. 8 Juxtaposition of optical (*left*) and fluorescent (*right*) micrographs of FITC-dextran loaded capsules **a** without AuNRs and **b** with AuNRs before and after 20 min NIR exposure. **c** Average fluorescence intensity profiles along the lines (shown in frame **b**) through the

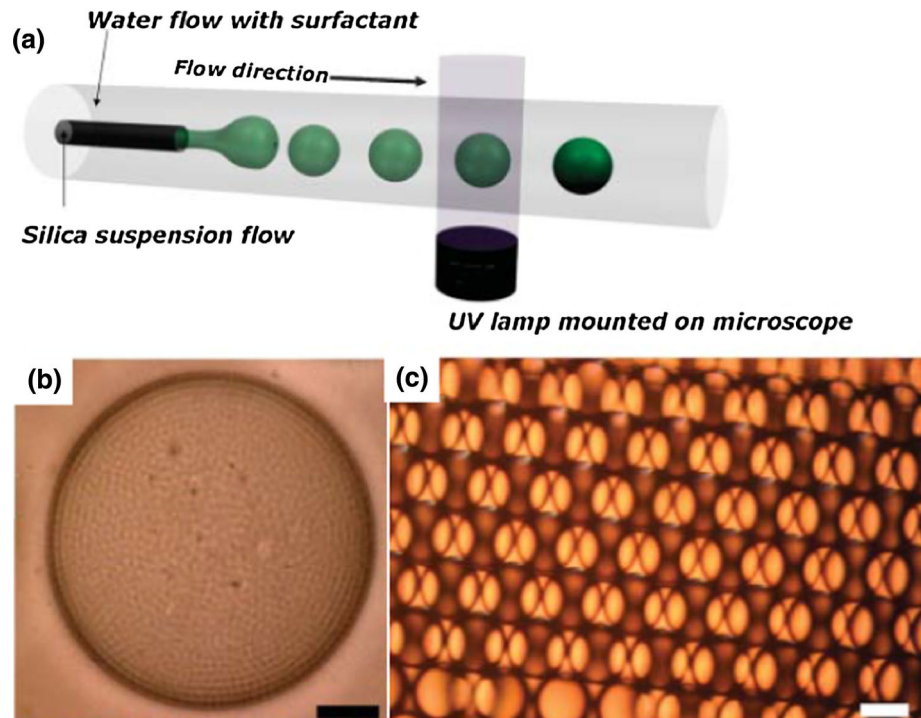
capsules **d** average fluorescence intensity from over 20 microcapsules (*error bars* represent the standard error of the mean). These images and graphs are adapted with permission from Lee et al. (2012). © 2012 Wiley-VCH Verlag GmbH & Co. KGaA

multiple monodisperse emulsion droplets. The droplets are decorated with a hexagonal array of silica particles and captured by rapid photopolymerization. The approach enables the silica particles to disperse through the droplet to the surface where they are anchored. The versatility of droplet microfluidics for synthesizing particles with simple to complex morphological and physical properties was further demonstrated by Kim et al. (2008) with the synthesis of monodisperse spherical photonic crystal balls using simple and high-throughput microfluidics devices. An index-matched precursor consisting of silica dispersed in ethoxylated trimethylolpropane triacrylate (ETPTA) suspension is used in a cocurrent flow system of two coaxial microcapillaries shown in Fig. 9a. Figure 9b shows a spherical silica-ETPTA composite photonic particle illustrating that the constituent silica particles layer in concentric spherical shells. The consolidated silica-ETPTA photonic particles reflect light at frequencies dependent on the particle size and volume fraction of the silica component (Fig. 9d). The superiority of droplet generation microfluidics is demonstrated in applications for controlled production of designer particles from single and double emulsion droplets and the manipulation and variation of experimental parameters (Jeong et al. 2012a, b).

5 Spheroidal polymeric particles

Spheroidal particles are particles with elliptical or platelet shapes. The synthesis, as well as applications, of spheroidal particles has been reviewed (Champion et al. 2007; Kuijk et al. 2011; Yang et al. 2008; Yin and Xia 2001) but is discussed here for completeness. In drug delivery, particle size is an important parameter; however, the shape is also critical. Decuzzi et al. (2010) reported that discoidal particles are observed to accumulate more than others in most of the organs but the liver, whereas cylindrical particles are deposited to a greater extent. This observation may support the notion that sub-micrometer discoidal particles can be used as intravascular carriers to maximize accumulation in the target organ, by suppressing their sequestration by the liver. Particle shape affects the transport, degradation, targeting, and internalization of drug delivery agents. While the motion of spheroidal particles in vessels is hindered by the shape as a result of tumbling and alignment and especially at bifurcations, their uptake in macrophage phagocytosis is important in targeted delivery (Champion et al. 2007; Kohane 2007; Mitragotri 2009). Microfluidics protocols for particle synthesis through droplet formation provides a platform to

Fig. 9 **a** Schematic illustration for the preparation of photonic balls of high monodispersity. **b** Cross-sectional image of a colloidal photonic ball of diameter 53.7 μm . The ball is composed of 1 μm silica particles embedded in an ETPTA matrix. **c** Optical microscopy images of monodisperse silica-in-ETPTA droplets. Scale bars **b** = 10 μm and **c** = 100 μm . This image is reproduced with permission from Kim et al. (2008). © 2008 Wiley-VCH Verlag GmbH & Co. KGaA



create particles of elongated structures which may enhance their cellular uptake.

Droplet formation in microfluidics devices is a unique platform toward synthesizing and controlling the structural parameters of spheroidal particles. In Flow-focus or T-junction capillary and PDMS devices, droplets can be deformed or strained depending on the channel geometry and the flow parameters. Xu et al. (2005) described microfluidics methods for producing monodisperse solid deformed spherical (spheroidal) particles in the size range of 20–1,000 μm . The method involves the formation of monodisperse liquid droplets using a microfluidic device and straining the droplets in the microchannels. The strained droplets are then solidified by photocrosslinking. The diameter and hence the shape of the droplets are controlled by manipulating the flow rates of the continuous and dispersed phases. In Fig. 10a, two immiscible liquids A and B are flowed into a narrow orifice where the inner liquid core breaks to release monodisperse droplets into the outlet channel. For thermal solidification experiments, the flow-focusing region was kept at a temperature exceeding the gelling (or solid–liquid phase transition) temperature (T_0). Figure 10a is a schematic of the flow-focus junction showing droplet formation, Fig. 10b, c illustrate the full device, Fig. 10d illustrates the formation of spherical particles, and Fig. 10e, f illustrate the formation of spheroidal particles. When the droplet size is not constrained by the channel, a spherical particle is produced. Otherwise, a spheroidal particle is produced. Figure 10g–j illustrates

particles synthesized using this approach. A similar approach is described by Dendukuri et al. (2005) but using a T-junction device illustrated in Fig. 11a. In this case, the droplets are first formed at the T-junction by shearing the photopolymer droplet, and then constraining to generate spheroidal shapes by confinement to the microchannel geometry. Example particles are shown in Fig. 11b, c. Shearing the polymer phase at low shear rates produced plug-like shapes, while disk-like shapes are obtained by flattening droplets using microchannels of reduced height. The approach enables the material properties of the particles to be altered using different photopolymers. Further, the particle size and morphology can be changed by manipulating the flow parameters of the precursor or the channel geometry.

6 Non-spherical, two-dimensionally extruded polymeric particles

In modern applications of micro- and nanoparticles, shape is as important as the size of the particles. For example, non-spherical particles have different behaviors from spherical particles under the same hydrodynamic (Brown et al. 2010), electric (Shum et al. 2010), and magnetic conditions (Solomon et al. 2010). However, the synthesis of non-spherical particles using conventional methods is tedious and can require the use of surfactants to manipulate crystallographic planes as well as account for surface

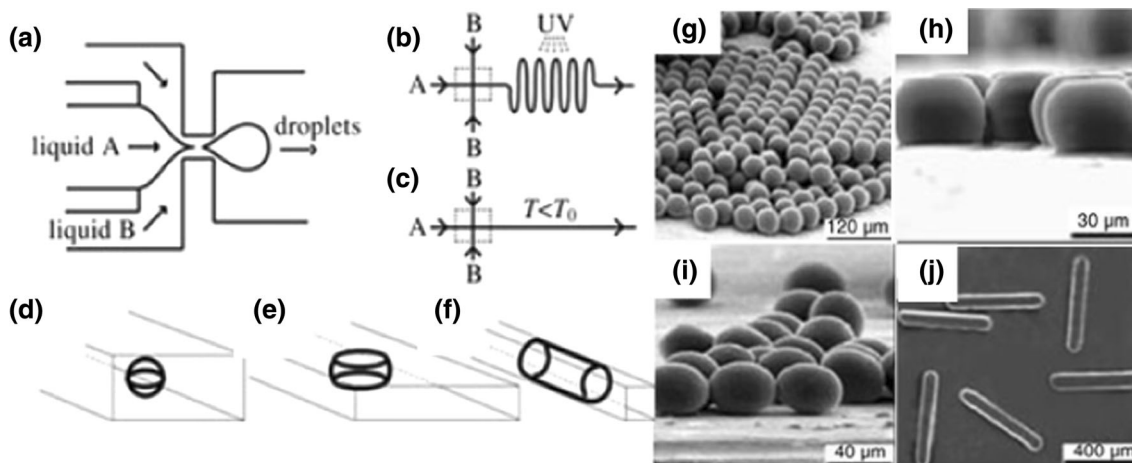


Fig. 10 **a** Schematic representation of the flow-focusing geometry used in the microfluidic droplet generation devices. **b** and **c** are line representations of the area of the devices for UV exposure to solidify particles. The *dashed rectangles* enclose the flow-focus junction. Representations **d–f** of the shapes of drops in the microfluidic channel. If the volume of the droplet exceeds that of the largest sphere

d which could be accommodated in the channel, the droplet is deformed into a **e** disk or **f** rod or ellipsoid. Optical microscopy images of poly(tri-propylene glycol diacrylate) (TPGDA) particles: **g** microspheres, **h** disks, **c** ellipsoids, and **j** rods. The figures are adapted with permission from Xu et al. (2005). © 2005 Wiley–VCH Verlag GmbH & Co. KGaA

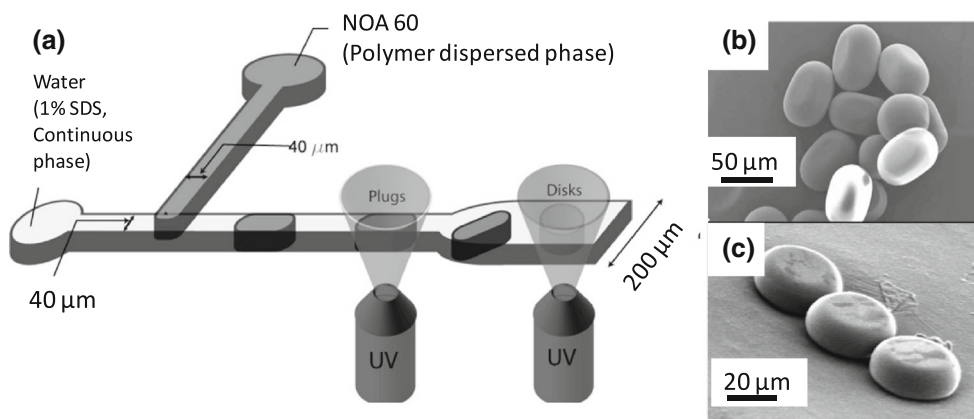


Fig. 11 **a** A T-junction device with constrained droplets exposed to UV downstream. **b–c** Micrographs of spheroidal particles formed based on the extent of droplet constraint after formation. The figures

are adapted with permission from Dendukuri et al. (2005). © 2011 American Chemical Society

energy requirements (Tao et al. 2008). Microfluidics, however, provides a platform to synthesize non-spherical particles whose shapes can be predetermined, and the technique also offers absolute control over particle size. The Doyle Group has played a pioneering role in the development of synthesizing non-spherical particles with two-dimensional extrusion using microfluidics also known as Stop-Flow Lithography (SFL). The method was previously illustrated in Fig. 3a–d. The state-of-the-art for SFL is automated SFL using a compressed-air flow control system (Bong et al. 2011; Dendukuri and Doyle 2009; Dendukuri et al. 2007; Baah et al. 2012). The particle synthesis and collection is made possible by the spontaneous free radical polymerization of a precursor reagent on

exposure to UV light of appropriate wavelength. The instant cessation of the reaction, once the UV source is removed, ensures high resolution with respect to particle cross-section. The permeability of PDMS devices to oxygen diffusion enables the immediate termination of the reaction which enables smooth ejection of synthesized particles without sticking to the device wall (Dendukuri et al. 2008). Once a photocrosslinkable precursor solution is constituted, particles of different cross-sectional shapes, functionality, composition, sizes, and aspect ratio can be synthesized. Chapin et al. (2011) used this method to synthesize encoded gel microparticles for rapid micro-RNA profiling. Further, the synthesis of cell laden microparticles with square, triangular, and circular cross-sections

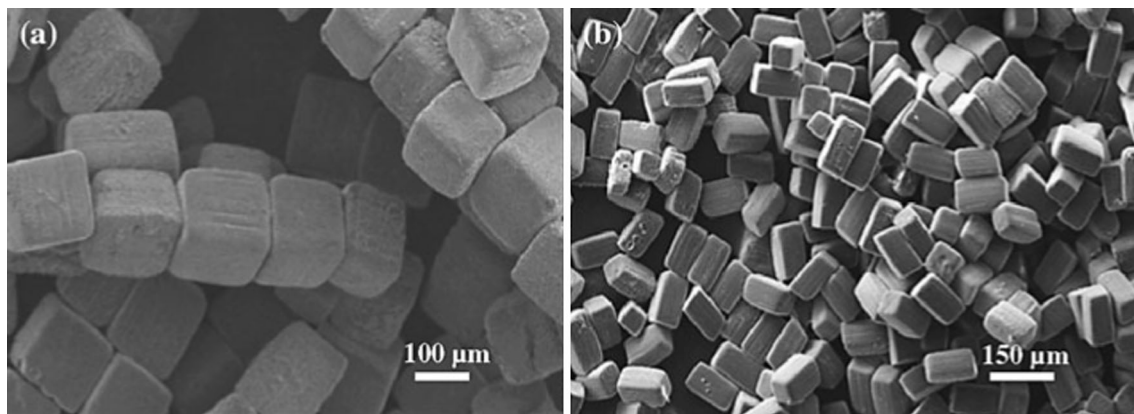


Fig. 12 **a** High-fidelity cubic PEGDA particles of $\sim 110 \mu\text{m}$ edge dimension formed using Stop-Flow Lithography, **b** Changing the objective magnification from $10\times$ (**a**) to $20\times$ creates high-aspect ratio particles. Image is adapted from Baah et al. (2012). © The Authors 2011

is reported by Panda et al. (2008). On post-synthesis analysis, the group found the majority of the encapsulated cells remained viable. Figure 3a–d illustrates how SFL enables particles to be synthesized with different cross-sectional shape, size, and composition. Further, Fig. 12 shows how particle size can be controlled by manipulating the magnification of the objective lens used in particle synthesis. In Fig. 12a, a $10\times$ objective is used to synthesize particles using a photomask with square pores. In Fig. 12b, a $20\times$ objective reduced the particle cross-section but the axial dimension and cross-sectional shape remain constant by keeping the channel depth and photomask fixed. The result is cubic particles in Fig. 12a and high-aspect ratio tetragonal particles in Fig. 12b demonstrated by simply changing the microscope objective. Other manipulated variables to control particle shape and size are the channel depth as well as the pore size in the photomask. It should be noted that one limitation of the PDMS device is solvent compatibility. Only polar precursor solvents work well with PDMS whereas nonpolar solvents swell the device. To address that shortcoming, a new device was developed (Bong et al. 2012) which is non-PDMS based and prevents oxygen diffusion through the device walls but has a solvent resistant enclave that allows the use of water insoluble precursors for particle synthesis.

Although SFL methods continue to be explored for the synthesis of polymeric, two-dimensionally extruded particles, Jang et al. (2007) reported a related, but distinctly different approach, Stop-Flow Interference Lithography (SFIL). A unique advantage of this method is that it does not necessarily make use of a patterned photo mask to define the cross-section of the particles. Instead, light interference can be used to define the cross-sectional shape of the particle and the 3-dimensional structure. SFIL is a combination of Stop Flow and Interference Lithography methods. An added advantage is the ability to repeatedly

flush out arrays of structured particles within seconds. The method is similar to the SFL method; however, in SFIL, a microfluidic device and phase mask are both fabricated or molded in PDMS and sealed to each other. When collimated light passes through the phase mask, a complex 3D pattern of light is created. This light pattern induces a free radical polymerization reaction of the oligomer. Figure 13 shows a schematic of the device (a), the experimental setup (b) and optical micrographs of representative particles (c–d).

7 Janus and other multiphase polymeric particles

Janus particles are generally described as a type of multiphase particle with two opposing faces. More technically, these are anisotropic particles with two components or chemically distinct phases which may give rise to surface activity and amphiphilic behavior (Jiang and Granick 2007; Wurm and Kilbinger 2009), cell targeting, fluorescence, and magnetic responses (Granick et al. 2009; Kaufmann et al. 2012; Seiffert et al. 2010). Conventionally, Janus particles are synthesized by self-assembly of block copolymers, competitive adsorption of mixtures of incompatible ligands, masking, droplets and pickering emulsion, and phase separation (Lattuada and Hatton 2011). Microfluidics techniques for particle synthesis are applicable to making two types of Janus particles; (1) spherical Janus particles and (2) two-dimensionally extruded Janus Particles. Multiphase microfluidics is rapidly advancing the synthesis of both types of Janus particles. For diffusion limited precursors, microemulsions formed at T-junction, Co-flow and Flow-focus junctions in capillary devices and laminar streams of precursors in PDMS devices can be transformed into particles with distinct phases. Figure 14a–e shows schematics of Janus and other

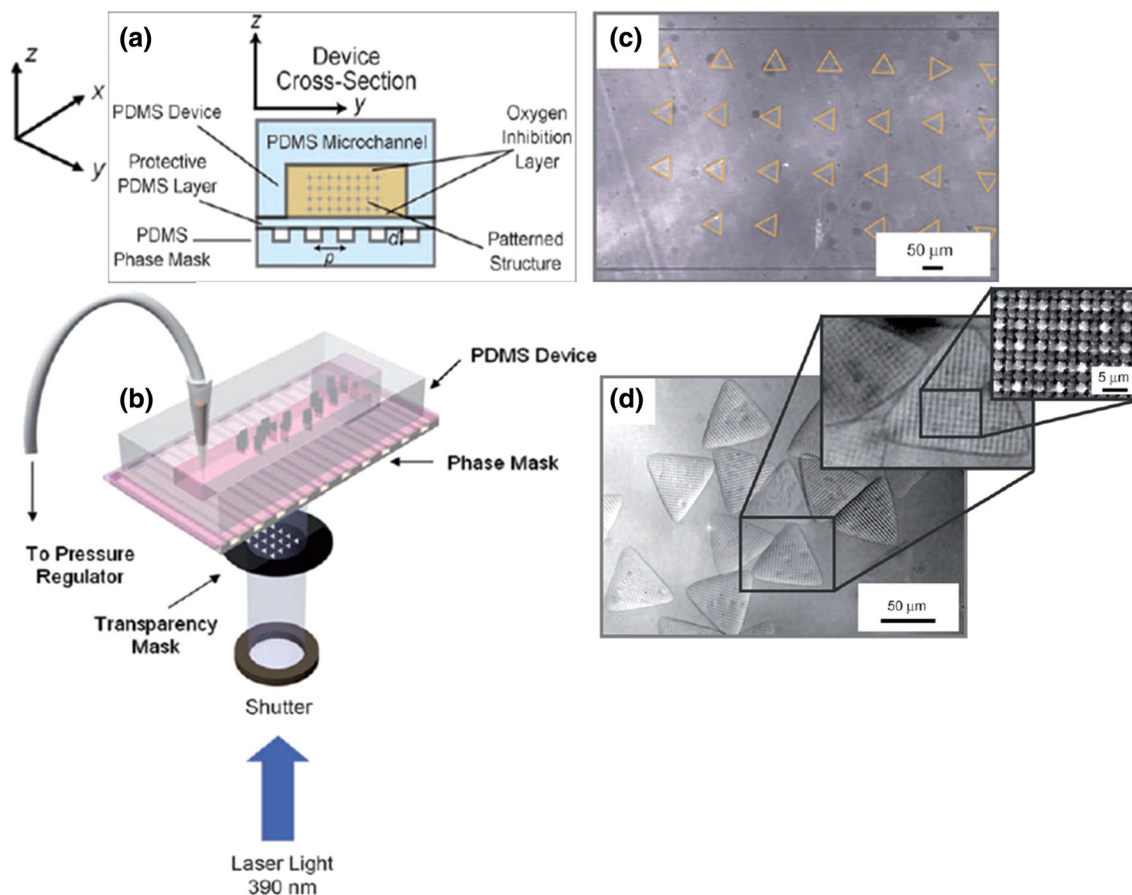


Fig. 13 **a** Schematic drawing of an SFIL PDMS microfluidic device integrated with a PDMS phase mask. **b** experimental setup for SFIL particle synthesis, **c** bright field image of an array of patterned triangular particles of side length $60\ \mu\text{m}$ formed in a $600\ \mu\text{m}$ wide and $30\ \mu\text{m}$ tall channel, **d** differential interference contrast image of triangular particles produced by SFIL shown in **c** after they have been

suspended in ethanol. A patterned grid-like structure formed by the phase mask is visible on the surface of the particles and seen more clearly in the inset SEM image. Images are adapted with permission from Jang et al. (2007). © 2007 Wiley-VCH Verlag GmbH & Co. KGaA

multiphase particles and their particle formation in both PDMS and capillary devices. A key requirement for successful fabrication of Janus particles is to keep the co-flowing streams parallel at all times. Any disturbance could result in cross-mixing of the fluids leading to the formation of near homogenous particles. Additionally, the interface between the two fluids must be stable and independent of both location and time (Chen et al. 2009). The synthesis of spherical but anisotropic particles of Poly(*N*-isopropylacrylamide) with dispersed ferromagnetic nanoparticles was reported by Seiffert et al. (2010). The particles have two distinguishable phases reflecting the composition of the precursor reagents. Also, Yuet et al. (2009) reported the synthesis of spherical Janus hydrogel particles, using the flow-focus method, with super-paramagnetic properties and chemical anisotropy. The particles are formed with a precursor constituted in PEG-DA ($M_n = 700$) and containing 3.6 wt% Fe_2O_3 nanoparticles (diameter = 9.8 nm), and their two-dimensional self-assembly is easily reorganized

into stable chainlike microstructures under an external magnetic field. It should be noted that the magnetic Fe_2O_3 nanoparticles are generated in situ. Using this method, biphasic, gradient, or homogenous magnetic particles have been synthesized.

SFL can also be used to synthesize Janus particles. For example, the controlled flow of two or more precursor streams from multiple inlets enables the fabrication of two-dimensionally extruded Janus particles (Fig. 15a). Such Janus particles composed of a fluorescent, graphically encoded region, and probe-loaded regions can be used to sensitively detect DNA oligomers in medical diagnostics (Cederquist et al. 2010; Pregibon et al. 2006). The authors intimated that the dot-coding pattern on the surface of the particles could include over a million codes (Fig. 15b–d). Figure 15e–g shows particles with a single-probe region, multiple-probe regions, and with probe regions in a gradient profile, respectively, synthesized by selectively labeling monomer streams with a fluorophore. In a report by Suh

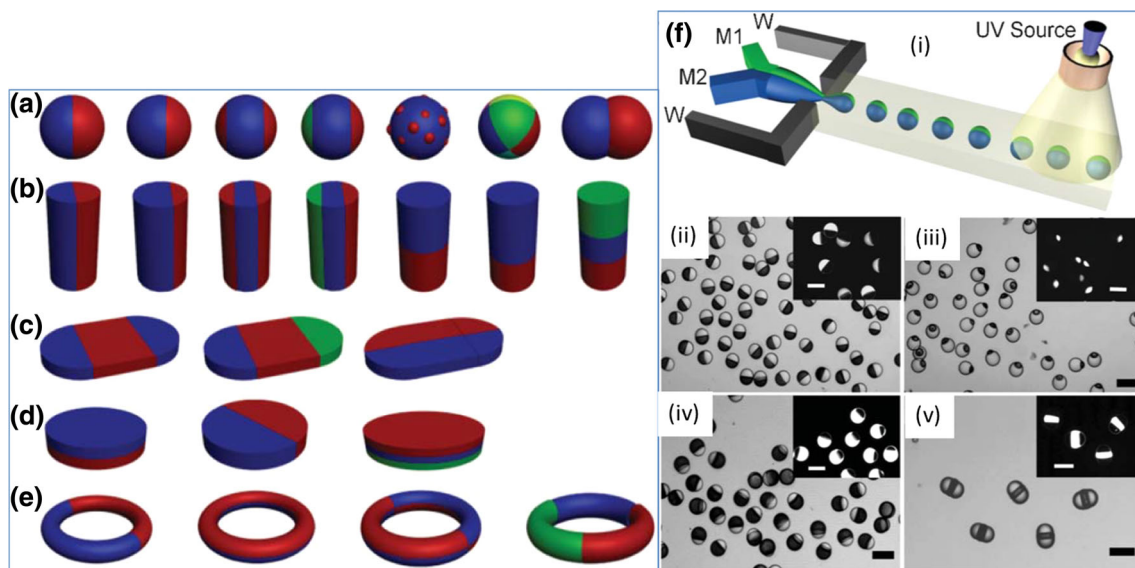


Fig. 14 Illustration of **a** zero, **b** one- and **c–e** two-dimensional Janus particles. Different colors represent different components of the particles. **f i** schematic of formation of droplets with ternary structures. **ii–iv** Optical microscopy images of Janus particles. Bright

and dark phases are polymers of M1 and M2, respectively. **v** Janus particles with ternary structures. The figures are adapted with permission from Yang et al. (2012) with permission. © 2012 Royal Society of Chemistry (color figure online)

et al. (2012) and using SFL, Janus particles are produced in non-spherical two-dimensionally extruded shapes. Figure 15h is a schematic illustration of a multi-inlet microfluidics device for synthesis of a more complex particle (Fig. 15i) tagged with fluorescent codes and probes useful for DNA profiling. The method demonstrates a combination of particle synthesis and encoding probe incorporation into a single process to generate biphasic or triphasic particles with multifunctionalities and over a million unique codes. The particles are used in multiplex fluorescence detection of DNA oligomers with encoded particles. The method offers a one step synthesis of particles useful for high-throughput screening in biological analysis.

8 Composite particles

Composite particles consist of an organic matrix in which inorganic nanoparticles are dispersed. An obvious advantage of the organic–inorganic system is the possible favorable combination of dissimilar properties of organic and inorganic components in one material for better performance. Further, it is possible to incorporate magnetic, inorganic particles in a polymer to synthesize multifunctional shape and size specific magneto-composite particles (Nunes et al. 2010). Polymer-nanocomposite particles are applied in devices such as photodiodes, gas sensors, light emitting diodes, optical and magnetic devices (Godovsky 2000), as well as in anticorrosive and antistatic applications (Hema et al. 2012). Predominantly, these composite

particles are of spherical shape with core–shell or homogeneous morphologies and have been synthesized using microemulsion polymerization (Chen et al. 2008; Negrete-Herrera et al. 2006; Qiang et al. 2008). Microfluidics technology for particle synthesis provides a means to synthesize both spherical and two-dimensionally extruded composite particles of different morphologies and sizes. In such synthesis applications, a precursor suspension of suitable viscosity, consisting of a base photocrosslinkable polymer with a dispersed inorganic nanofiller is required.

In 2006, Shepherd et al. (2006) reported the synthesis of homogeneous and Janus colloid-filled hydrogel granules. First, a colloidal suspension of SiO₂ (500 nm) in acrylamide and *N,N*-methylenebisacrylamide with 2,2-diethoxyacetophenone as the photoinitiator was prepared and flowed through a flow-focus device using oil as the continuous phase. The droplets were exposed to UV after their formation to create particles in the range of 80–95 μm. In a similar approach, the UV light can be filtered with a patterned photomask and focused onto a stream of the precursor to create two-dimensionally extruded particles. Figure 16 shows micrographs of composite particles of nano-SiO₂/PEG-DA with different cross-sectional shapes, sizes and designs (Baah et al. 2013) synthesized using SFL. Baah et al. (2013) also demonstrated the synthesis of nano-Al₂O₃/PEG-DA particles using SFL. A patterned photomask controls the cross-sectional shape, while the size is controlled using different objective lens and channel depth devices. For example, the size reduction from Fig. 16a, b is achieved by switching a 10× magnification objective lens

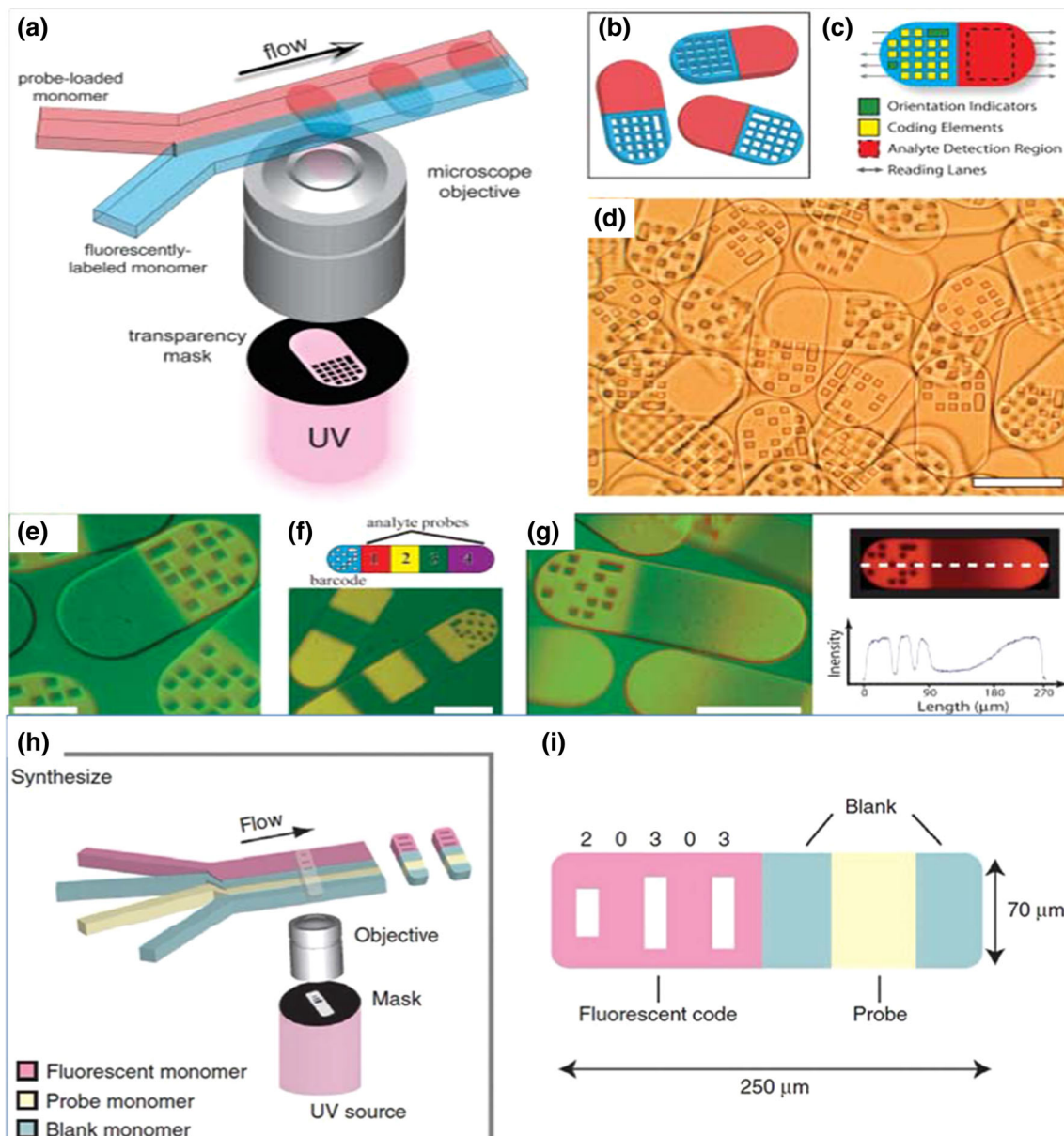


Fig. 15 **a** Schematic diagram of dot-coded particle synthesis showing polymerization across two adjacent laminar streams to make single-probe, half-fluorescent particles (shown in **b**). **c** Diagrammatic representation of particle features for encoding and analyte detection. The encoding scheme shown allows the generation of 220 (1,048,576) unique codes. **d** Differential interference contrast (DIC) image of particles generated using the scheme shown in **a**. **e** Overlap of fluorescence and DIC images of **e** single-probe, **(f, bottom)** multi-

probe, and probe-gradient (**g, left**) encoded particles. Shown also is a schematic representation of multi-probe particles (**f, top**) and a plot of fluorescent intensity along the center line of a gradient particle (**g, right**). Scale bars indicate 100 μm in **d, f,** and **g** and 50 μm in **e**. Images are adapted with permission from Pregibon et al. (2006). **h** schematic diagram of the synthesis of single-probe particles. **i** bar-coded particle with code 20303. Images are adapted with permission from Yang et al. (2012). © The Royal Society of Chemistry 2012

to a 20 \times . This resulted in a reduction in the cross-sectional dimensions. The axial dimensions are reduced by using a shallower channel. Similar size reductions were achieved from Fig. 16c, d. Figure 16e, f further demonstrate the range of two-dimensionally extruded particles that can be synthesized with the demonstration of particles with vias.

In addition to synthesizing passive composite particles, the synthesis of magnetic hydrogel particles (consisting of magnetic beads dispersed in PEG-DA) has been reported (Suh et al. 2012). The particles fabricated in two-dimensional extrusion and of low aspect ratio are magnetic and have both code and probe making them suitable for a

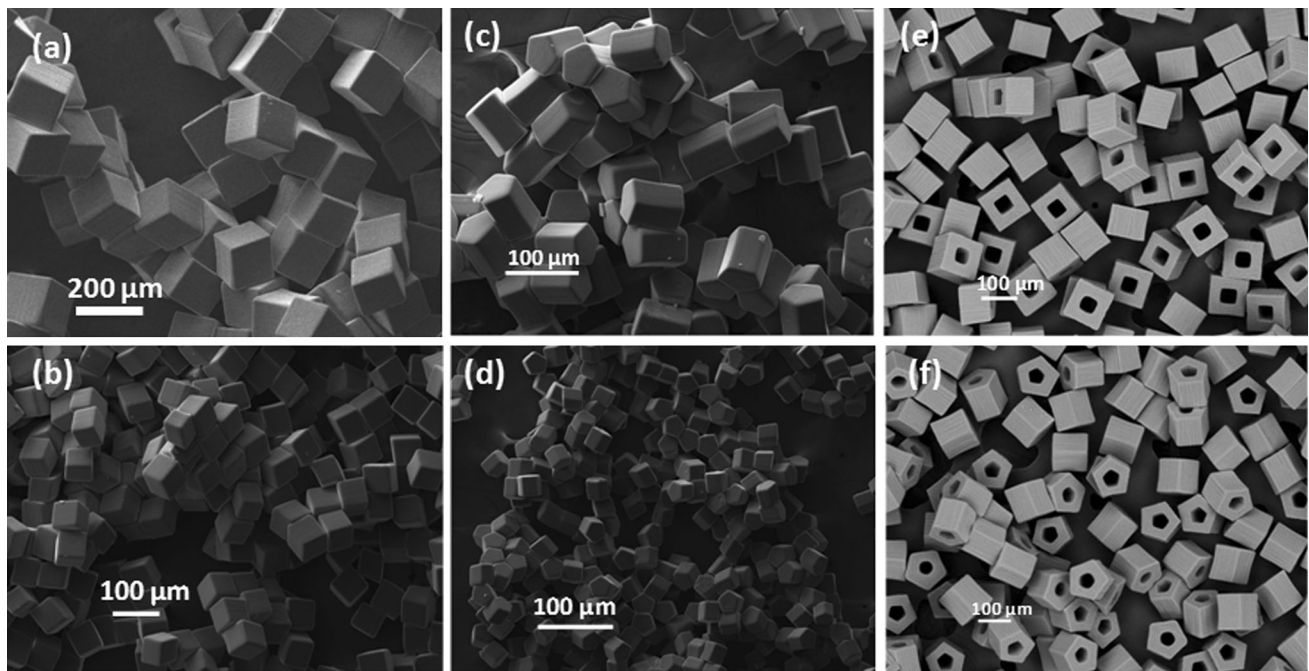


Fig. 16 Scanning Electron Micrographs of composite particles (nanosized SiO₂ particles dispersed in PEGDA) demonstrating size reduction and change in *shapes*. **b** and **d** Are the respective reduced

sizes of **a** and **c**. Particles of square (**e**) and pentagonal (**f**) cross-sections with *square* and *pentagonal* vias, respectively

multiplex assay. The ability of the particle to combine the magnetic functionality with both coding and target capture within the same bar-coded region was demonstrated for microRNA detection.

Finally, when discussing synthesis of composite particles, it is important to mention that the suitability of the inorganic/organic suspension for photocrosslinking is dependent on its index-match state. An index-matched suspension allows UV light to pass with minimal diffraction interference so that the photopolymer can be cross-linked. Therefore, a limitation of this method is the reflection of UV–Vis light due to the presence of highly refractive inorganic material. For a direct dispersion of the inorganic nanofiller into the base polymer, the preparation of stable precursor requires matching the index of refraction of the particles to that of the suspending medium. Alternatively, a precursor can be prepared by diluting a concentrated index-matched suspension of the nanofiller of interest (e.g., Ludox[®]—a commercial dispersion of SiO₂ in aqueous medium). In addition to index matching, one should consider the viscosity of the precursor suspension which increases significantly with the addition of nanoparticles.

9 Ceramic and metallic particles

The application of microfluidics technology for particle synthesis goes beyond the synthesis of particles consisting

of thermal and photocrosslinkable polymers and their composites. For over a decade, it has been possible to mimic the conventional sol–gel, hydrothermal, hydrolysis, redox, and precipitation reactions and methods of particle synthesis in microfluidic channels to generate monodisperse metallic and metal oxide particles (Marre and Jensen 2010; Abou-Hassan et al. 2010; Zhao et al. 2011). The microfluidic platform offers better control over solution dispensing and mixing leading to improved control over nucleation and particle growth resulting in highly monodisperse particles of largely spherical particles. Khan et al. (2004) suggested that for any laminar flow design of particle synthesis microreactor, high particle monodispersity is only achievable under conditions of minimum axial dispersion. The group designed a segmented flow microreactor (Fig. 17a) which not only ensures the production of monodisperse particles by minimizing axial dispersion effects, but is also a useful tool for generating kinetic data. Wacker et al. (2012) formed particles from precursor droplets generated at a flow-focus junction. The droplets were generated by a laminar flow of tetraethyl orthosilicate (TEOS)-ethanol, tagged with Fluorescein-isothiocyanate (FITC) and ammonia-ethanol in a Fluorinert oil continuous phase (Fig. 17b). FITC is coupled to APTES and mixed off-chip with TEOS to yield a fluorescent silicon alkoxide solution (SA). A hydrolyzing mixture (HM) and SA are injected into the microfluidic chip, where they are merged and converted into a stream of droplets in Fluorinert oil

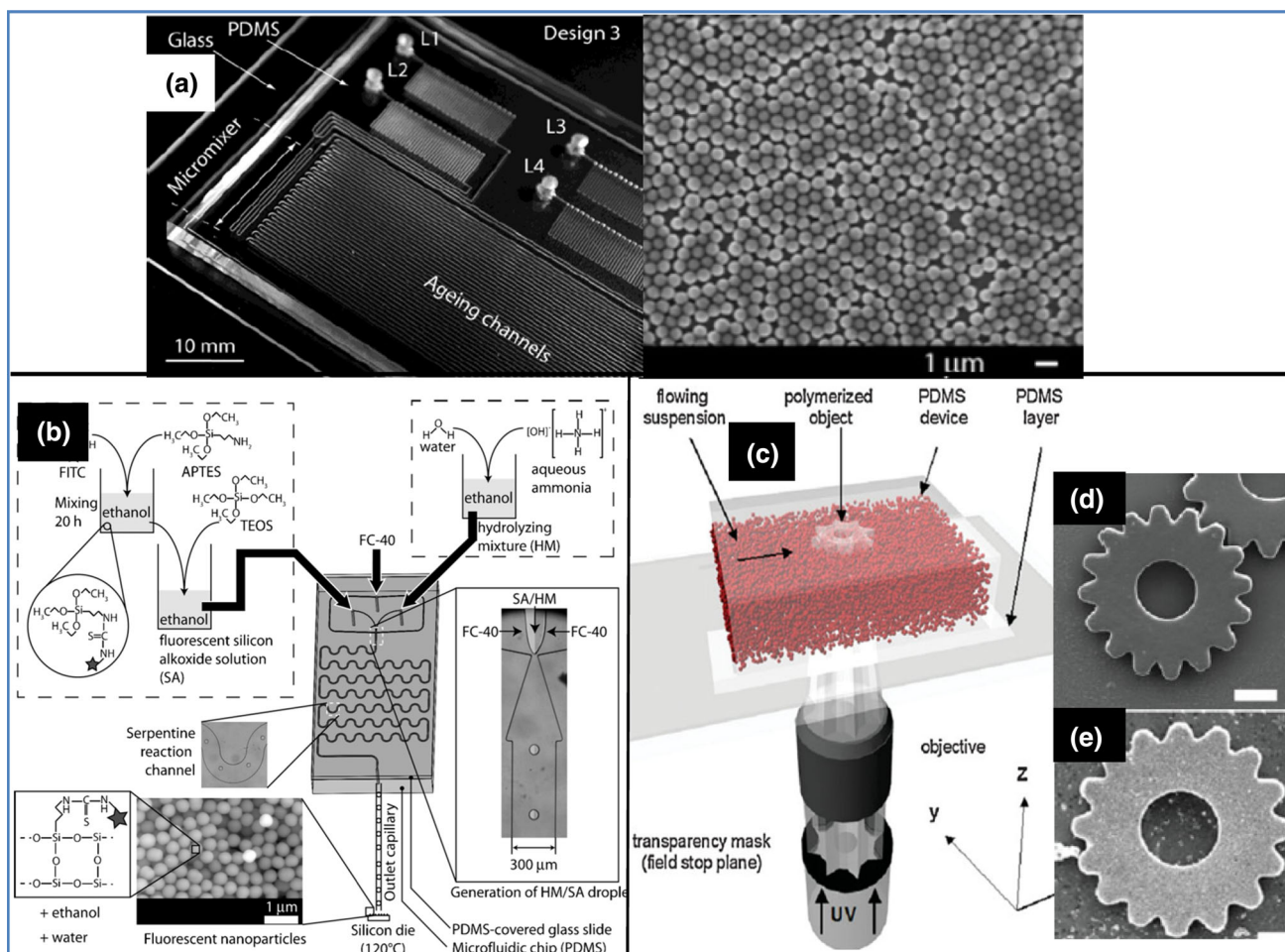


Fig. 17 **a** Photograph of segmented flow microreactor (Design 3): L1–L4 are the liquid inlets. Adjacent is a low magnification SEM of SiO_2 particles of ~ 540 nm in size with dispersity of 4.5 %. The figure is adapted with permission from Khan et al. (2004). © 2004 American Chemical Society. **b** Procedure and apparatus for the droplet-based synthesis of fluorescent SiO_2 nanoparticles. The figure is adapted from Wacker et al. (2012). © 2012 The Royal Society of Chemistry. **c** Schematic illustration of stop-flow lithography (SFL)

system, where a photocurable, index-matched silica-acrylamide suspension is flowed through a PDMS microchannel and exposed to UV light on stoppage. **d** SEM micrograph of a glassy silica microgear fully densified at $1,150^\circ\text{C}$ for 10 h. **e** SEM micrograph of a porous silicon microgear converted by a magnesiothermic reduction in the silica microgear. The Figures are adapted from Shepherd et al. (2008). © 2008 WILEY-VCH Verlag GmbH & Co. KGaA, Weinheim

(FC-40) by a flow-focusing nozzle. After evaporation of the reagents, the SiO_2 nanoparticles are analyzed by electron microscopy. The approach, which offers excellent control over reagent concentration and reaction time, yields SiO_2 nanoparticles of ~ 350 nm and 3 % dispersity. This observation is consistent with that of Yang et al. (2010) who used the microfluidic platform to investigate size controlled synthesis of gold nanoparticles. Notably, in a different study, controlling reaction time and reagent concentration, as well as using quenching techniques, yields three distinct crystal structures of Co nanoparticles (Song et al. 2006).

While the methods discussed above do not involve the use of photopolymerization, they are, nonetheless, useful for direct preparation of spherical ceramic particles and

provide a basis for comparison with microfluidics methods that use photocrosslinkable materials to indirectly synthesize non-spherical ceramic and metallic particles. While it is straightforward to directly synthesize spherically shaped ceramic particles in microfluidics reactors, the same cannot be said of two-dimensionally extruded particles due to constraints imposed by the particle formation reaction. Thus, indirect methods like SFL are employed. In an early demonstration of SFL for preparation of ceramic and metallic particles, Shepherd et al. (2008) fabricated a porous Si microgear using the Stop-Flow Lithography method. In their method, as illustrated in Fig. 17c a suspension of SiO_2 in polyethyleneimine was prepared and then transformed into composite particles via in situ photopolymerization using SFL. The composite particles were

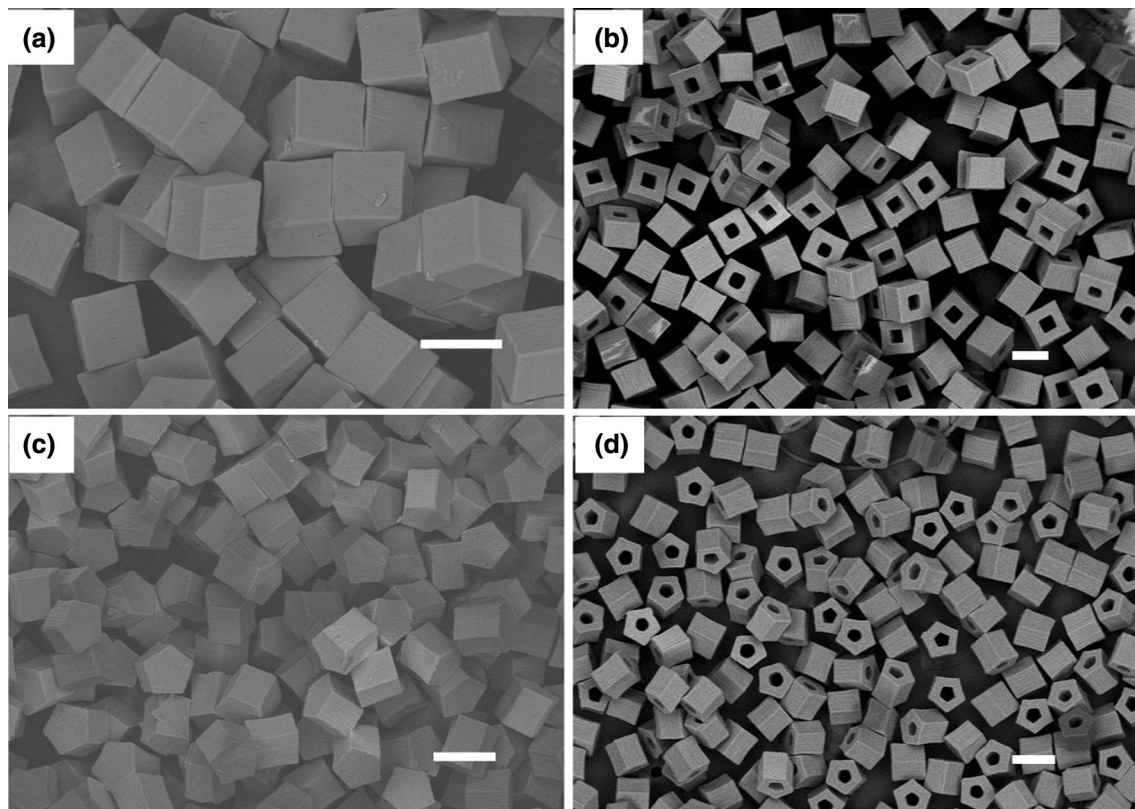


Fig. 18 Indirect Stop-Flow Lithography SiO_2 particles in *square* and *pentagonal* cross-sectional shapes with and without vias prepared by sintering composite particles to remove binder and consolidate inorganic nanoparticles. Scale bar 100 μm

subsequently heated to 1,150 $^\circ\text{C}$ for approximately 10 h to form SiO_2 microparticles (gears) shown in Fig. 17d. Next, further heating of the SiO_2 in the presence of Mg gas facilitated the transformation of SiO_2 to porous Si shown in Fig. 17e. Additionally, Baah et al. (2013) demonstrated the synthesis of SiO_2 and Al_2O_3 particles by first synthesizing composite particles using SFL techniques previously described. After synthesis, the composite particles were heated to 600 $^\circ\text{C}$ to remove the polymer binder and finally heated to 1,150 $^\circ\text{C}$ to consolidate the SiO_2 nanoparticles and 1,450 $^\circ\text{C}$ to consolidate the Al_2O_3 nanoparticles. The composition of the consolidated particles was confirmed using X-ray Diffraction (XRD). The results indicated the synthesis of Cristobalite (SiO_2) and Corundum (Al_2O_3). Figure 18 shows scanning electron micrographs of ceramic SiO_2 particles obtained from the composite analogues through sintering as described above. Both solid particles and particles with single through vias have been demonstrated.

When inorganic particles are indirectly obtained from the composite (polymer + inorganic) particles, the final particle size is determined by the filler loading (Baah et al. 2013). In principle, sub-micron particles could be achieved by using very low particle loadings. The difficulty is that at

particle loadings below 10 wt%, the particles can collapse when sintered and therefore not retain their original shape.

10 Particle throughput

In spite of the versatility of microfluidics for particle synthesis from photocrosslinkable materials, commercial acceptance of the method is dependent on the particle yield. Therefore, the focus of the applied research community is to engage engineering ingenuity to scale up particle production in order to facilitate the transfer of the technology from lab demonstration into full scale commercialization. The synthesis of spherical and pseudo-spherical particles using droplets as precursors has seen faster progress in terms of commercialization activities with Companies like Dolomite making tremendous progress in device and pump manufacturing. Droplet formation rates in excess of 10,000 per second have been reported. With an array of 16 droplet generators, droplets of 140 μm in diameter are generated at rates that translate into nearly 50 g of particles per hour (Li et al. 2009). Other investigators have corroborated the multiplicity of droplet generators as a means of enhancing the throughput of

microfluidics synthesis of spherical particles (Mulligan and Rothstein 2012).

While channel multiplicity for droplet generators is an option for scale-up, the same cannot be said of the SFL. SFL relies on making an array of particles per light exposure. The size of the array is dependent on the microscope field of view. From the authors' experience, achieving good particle resolution limits synthesis to a 5×5 particle array using an Olympus BX51 microscope. It is important to note with spherical particles, droplets are completely suspended in or enveloped in the solvent. In contrast, SFL particles require the patterned light to be focused at the fluid-device interface in order to clearly define the particle cross-sectional shape. This potentially deteriorates the PDMS device after several exposures at the same spot. Consequently, this requires the exposure spot to be moved after approximately 30 min of continuous exposure; otherwise, the particles may stick and clog the device. An uninterrupted synthesis will improve particle throughput. However, in spite of the challenges, production rates of 0.2 g per hour for 50 μm particles have been reported for SFL (Dendukuri and Doyle 2009).

11 Summary and outlook

In this paper, microfluidics for synthesis of particles from photocrosslinkable materials was reviewed. The paper emphasized that hydrogels are the materials of choice because they are water soluble and the photopolymerization kinetics are fast. Two types of devices, PDMS and glass capillary devices, are typically employed. Additionally, two methods, one which relies on droplet formation and another, referred to as stop-flow lithography, are preferred. Finally, a range of particles including spherical, spheroidal, Janus, composite and metal or metal oxide have been demonstrated.

Clearly, opportunities exist with microfluidics technology to synthesize high-fidelity particles of uniform dispersion from photocrosslinkable materials. Although throughput has been flagged as an area of improvement, the authors consider that area applied research within the domain of companies like Firefly Bioworks and, perhaps, academic engineering research centers. Future fundamental research should be concentrated in the area of SFL and include demonstration of sub-micron particles, investigation of additional particle compositions and use of the particles in niche applications.

Applications in the area of nanotechnology would be enabled by the demonstration of the synthesis of custom-made sub-micron particles using the SFL method. Such an achievement is dependent on reduced channel dimensions, reduced geometric feature sizes in the photomask, higher

objective magnification and lower particle loading for metal oxide particles. The device channel depth controls the axial dimension of the particles. Therefore, reduced channel depths would produce particles of low axial dimensions. The particle cross-sectional dimension is dependent on the geometric feature size in the photomask and objective magnification. It should be noted, however, that, as the feature dimensions near the wavelength of visible light, diffraction could be observed. Higher objective magnifications may complement a reduced photomask pore size to achieve particle cross sections with sub-micron dimensions. A possible challenge with these specifications is that the smaller-sized particles may be difficult to separate from unreacted precursor. For the ceramic particles, additional size reduction could be achieved by lowering the inorganic nanoparticle loading. However, a threshold particle loading concentration needs to be established for specific nanoparticles. Below this threshold loading, the particle shape may not be retained. This phenomenon is believed to be largely due to excessive void volume as the binder is removed during the heat treatment. The long-range inter-particle connection is too weak to hold the structure together.

The synthesis of other inorganic particles would be interesting as it would open opportunities for satisfying structural application requirements. However, most of the transition metal oxides (e.g., TiO_2 , ZnO , ZrO_2 , etc.) are inherently UV screening and their opaque suspensions are not compatible with SFL. It is recommended that constituting optically transparent suspensions be the priority, but translucent solutions could also be investigated. These suspensions are commercially available, especially those of SiO_2 and Al_2O_3 .

Modern applications of suspensions of colloidal particles are largely connected to the design of morphological features for such particles. For example, (Barua et al. 2013) investigated spherical and non-spherical micro- and nanoparticles for their specific binding interaction with cells. Their report indicated that for specific and non-specific uptake in three breast cancer cell lines: BT-474, SK-BR-3, and MDA-MB-231, rod-shaped particles exhibited higher specific uptake and lower non-specific uptake in all cells compared with spheres. Additionally, trastuzumab-coated rods exhibited greater inhibition of BT-474 breast cancer cell growth in vitro to a level unattainable by soluble forms of the antibody. These results reinforce earlier reports on the importance of particle shape in drug delivery (Champion et al. 2007; Mitragotri 2009), and reveal unique opportunities for particulate forms of antibodies in therapeutics and diagnostics.

Spherical inorganic metal oxide particles, particularly those of SiO_2 , are widely investigated for their shear thickening properties in oligomer systems (Hassan et al.

2010; Kalman and Wagner 2009; Lee and Wagner 2003; Raghavan and Khan 1997). This shear thickening behavior is shown to have a contemporary practical application in liquid body armor for ballistic protection (Decker et al. 2007; Lee et al. 2003; Li et al. 2008). Even though theoretical studies (Barnes 1989) have shown that non-spherical particles are better at inducing shear thickening, the synthesis of such particles is difficult with conventional methods. However, it may be possible to use microfluidics techniques to synthesize non-spherical particles in the range of 100–700 nm which falls within the ideal range of particle sizes for shear thickening (Barnes 1989). In addition to rheological studies, the particles described in this review may have applications in other fundamental studies that investigate the role of particle shape.

Acknowledgments This work was supported by the US Department of Energy under award number DE-SC0002470 and by the National Science Foundation under award number DMR-0611612. David Baah gratefully acknowledges a graduate fellowship from Alabama EPSCoR.

References

- Abate AR, Weitz DA (2011) Syringe-vacuum microfluidics: a portable technique to create monodisperse emulsions. *Biomicrofluidics* 5(1):014107–014108
- Abate AR, Krummel AT, Lee D, Marquez M, Holtze C, Weitz DA (2008) Photoreactive coating for high-contrast spatial patterning of microfluidic device wettability. *Lab Chip* 8(12):2157–2160
- Abate AR, Thiele J, Weitz DA (2010) One-step formation of multiple emulsions in microfluidics. *Lab Chip* 11(2):253–258
- Abou-Hassan A, Sandre O, Cabuil V (2010) Microfluidics in Inorganic Chemistry. *Angew Chem Int Ed* 49(36):6268–6286
- Alveroglu E, Sozeri H, Baykal A, Kurtan U, Senel M (2013) Fluorescence and magnetic properties of hydrogels containing Fe₃O₄ nanoparticles. *J Mol Struct* 1037:361–366
- Baah D, Vickers D, Hollinger A, Floyd-Smith T (2008) Patterned dispersion of nanoparticles in hydrogels using microfluidics. *Mater Lett* 62(23):3833–3835
- Baah D, Tigner J, Bean K, Britton B, Walker N, Henderson G, Floyd-Smith T (2011) Preparation of planar graded refractive index nanocomposites using microfluidics. *Mater Sci Eng, B* 176(12):883–888
- Baah D, Tigner J, Bean K, Walker N, Britton B, Floyd-Smith T (2012) Microfluidic synthesis and post processing of non-spherical polymeric microparticles. *Microfluid Nanofluid* 12(1–4):657–662
- Baah D, Donnell T, Tigner J, Floyd-Smith T (2013) Stop flow lithography synthesis of non-spherical metal oxide particles. *Particuology*. doi:10.1016/j.partic.2013.09.001
- Barnes H (1989) Shear-thickening ('Dilatancy') in suspensions of nonaggregating solid particles dispersed in Newtonian liquids. *J Rheol* 33(2):329–366
- Baroud CN, Gallaire F, Dangla R (2010) Dynamics of microfluidic droplets. *Lab Chip* 10(16):2032–2045
- Barua S, Yoo J-W, Kolhar P, Wakankar A, Gokarn YR, Mitragotri S (2013) Particle shape enhances specificity of antibody-displaying nanoparticles. *Proc Natl Acad Sci* 110(9):3270–3275
- Beebe DJ, Moore JS, Bauer JM, Yu Q, Liu RH, Devadoss C, Jo B-H (2000) Functional hydrogel structures for autonomous flow control inside microfluidic channels. *Nature* 404(6778):588–590
- Bong KW, Bong KT, Pregibon DC, Doyle PS (2010) Hydrodynamic focusing lithography. *Angew Chem* 122(1):91–94
- Bong KW, Chapin SC, Pregibon DC, Baah D, Floyd-Smith TM, Doyle PS (2011) Compressed-air flow control system. *Lab Chip* 11(4):743–747
- Bong KW, Xu J, Kim J-H, Chapin SC, Strano MS, Gleason KK, Doyle PS (2012) Non-polydimethylsiloxane devices for oxygen-free flow lithography. *Nat Commun* 3:805
- Brown E, Forman NA, Orellana CS, Zhang H, Maynor BW, Betts DE, DeSimone JM, Jaeger HM (2010) Generality of shear thickening in dense suspensions. *Nat Mater* 9(3):220–224
- Burdick JA, Peterson AJ, Anseth KS (2001) Conversion and temperature profiles during the photoinitiated polymerization of thick orthopaedic biomaterials. *Biomaterials* 22(13):1779–1786
- Burdick JA, Khademhosseini A, Langer R (2004) Fabrication of gradient hydrogels using a microfluidics/photopolymerization process. *Langmuir* 20(13):5153–5156
- Cederquist KB, Dean SL, Keating CD (2010) Encoded anisotropic particles for multiplexed bioanalysis. *Wiley Interdiscip Rev Nanomed Nanobiotechnol* 2(6):578–600
- Champion JA, Katare YK, Mitragotri S (2007) Particle shape: a new design parameter for micro- and nanoscale drug delivery carriers. *J Control Release* 121(1–2):3–9
- Chapin SC, Appleyard DC, Pregibon DC, Doyle PS (2011) Rapid microRNA profiling on encoded gel microparticles. *Angew Chem* 123(10):2337–2341
- Cheah LT, Fritsch I, Haswell SJ, Greenman J (2012) Evaluation of heart tissue viability under redox-magnetohydrodynamics conditions: toward fine-tuning flow in biological microfluidics applications. *Biotechnol Bioeng* 109(7):1827–1834
- Chen JH, Cheng CY, Chiu WY, Lee CF, Liang NY (2008) Synthesis of ZnO/polystyrene composites particles by Pickering emulsion polymerization. *Eur Polym J* 44(10):3271–3279
- Chen CH, Shah RK, Abate AR, Weitz DA (2009) Janus particles templated from double emulsion droplets generated using microfluidics. *Langmuir* 25(8):4320
- Choi C-H, Jung J-H, Hwang T-S, Lee C-S (2009) In situ microfluidic synthesis of monodisperse PEG microspheres. *Macromol Res* 17(3):163–167
- Chung CK, Shih TR, Chang CK, Lai CW, Wu BH (2011) Design and experiments of a short-mixing-length baffled microreactor and its application to microfluidic synthesis of nanoparticles. *Chem Eng J* 168(2):790–798
- Cowie JMG, Arrighi V (2008) *Polymers: chemistry and physics of modern materials*. J.M.G. Cowie, Valeria Arrighi. CRC Press, Boca Raton, FL
- Decker MJ, Halbach CJ, Nam CH, Wagner NJ, Wetzel ED (2007) Stab resistance of shear thickening fluid (STF)-treated fabrics. *Compos Sci Technol* 67(3–4):565–578
- Decuzzi P, Godin B, Tanaka T, Lee SY, Chiappini C, Liu X, Ferrari M (2010) Size and shape effects in the biodistribution of intravascularly injected particles. *J Control Release* 141(3):320–327
- Dendukuri D, Doyle PS (2009) The synthesis and assembly of polymeric microparticles using microfluidics. *Adv Mater* 21(41):4071–4086
- Dendukuri D, Tsoi K, Hatton TA, Doyle PS (2005) Controlled synthesis of nonspherical microparticles using microfluidics. *Langmuir* 21(6):2113–2116
- Dendukuri D, Gu SS, Pregibon DC, Hatton TA, Doyle PS (2007) Stop-flow lithography in a microfluidic device. *Lab Chip* 7(7):818–828
- Dendukuri D, Panda P, Haghgooe R, Kim JM, Hatton TA, Doyle PS (2008) Modeling of oxygen-inhibited free radical photopolymerization in a PDMS microfluidic device. *Macromolecules* 41(22):8547–8556

- Diao Y, Helgeson ME, Myerson AS, Hatton TA, Doyle PS, Trout BL (2011) Controlled nucleation from solution using polymer microgels. *J Am Chem Soc* 133(11):3756–3759
- Dong PF, Xu JH, Zhao H, Luo GS (2013) Preparation of 10 micron scale monodispersed particles by jetting flow in coaxial microfluidic devices. *Chem Eng J* 214:106–111
- Duncanson WJ, Lin T, Abate AR, Seiffert S, Shah RK, Weitz DA (2012) Microfluidic synthesis of advanced microparticles for encapsulation and controlled release. *Lab Chip* 12(12):2135–2145
- Fouassier JP, Allonas X, Burget D (2003) Photopolymerization reactions under visible lights: principle, mechanisms and examples of applications. *Prog Org Coat* 47(1):16–36
- Giridharan V, Yun Y, Hajdu P, Conforti L, Collins B, Jang Y, Sankar J (2012) Microfluidic platforms for evaluation of nanobiomaterials: a review. *J Nanomater* 2012:14. doi:10.1155/2012/789841
- Godovsky DY (2000) Device applications of polymer-nanocomposites. In: *Biopolymers A-PVA hydrogels, anionic polymerisation nanocomposites*, vol 153. *Advances in Polymer Science*. Springer, Berlin, pp 163–205
- Gokmen MT, Du Prez FE (2012) Porous polymer particles—a comprehensive guide to synthesis, characterization, functionalization and applications. *Prog Polym Sci* 37(3):365–405
- Golden J, Justin G, Nasir M, Ligler F (2012) Hydrodynamic focusing—a versatile tool. *Anal Bioanal Chem* 402(1):325–335
- Granick S, Jiang S, Chen Q (2009) Janus particles. *Phys Today* 62(7):68–69
- Gratton SEA, Pohlhaus PD, Lee J, Guo J, Cho MJ, DeSimone JM (2007) Nanofabricated particles for engineered drug therapies: a preliminary biodistribution study of PRINT nanoparticles. *J Control Release* 121(1–2):10–18
- Gratton SEA, Williams SS, Napier ME, Pohlhaus PD, Zhou Z, Wiles KB, Maynor BW, Shen C, Olafsen T, Samulski ET, DeSimone JM (2008) The pursuit of a scalable nanofabrication platform for use in material and life science applications. *Acc Chem Res* 41(12):1685–1695
- Gu H, Duits MHG, Mugele F (2011) Droplets formation and merging in two-phase flow microfluidics. *Int J Mol Sci* 12(4):2572–2597
- Hassan TA, Rangari VK, Jeelani S (2010) Sonochemical synthesis and rheological properties of shear thickening silica dispersions. *Ultrason Sonochem* 17(5):947–952
- Helgeson ME, Chapin SC, Doyle PS (2011) Hydrogel microparticles from lithographic processes: novel materials for fundamental and applied colloid science. *Curr Opin Colloid Interface Sci* 16(2):106–117
- Hema B, Kumar SA, Dhawan SK (2012) Conducting polymer nanocomposites for anticorrosive and antistatic applications. *Nanocompos N Trends Dev*. <http://dx.doi.org/10.5772/50470>
- Ifkovits JL, Burdick JA (2007) Review: photopolymerizable and degradable biomaterials for tissue engineering applications. *Tissue Eng* 13(10):2369–2385
- Jang J-H, Dendukuri D, Hatton TA, Thomas EL, Doyle PS (2007) A route to three-dimensional structures in a microfluidic device: stop-flow interference lithography. *Angew Chem Int Ed* 46:9027–9041
- Jeong W-C, Choi M, Lim CH, Yang S-M (2012a) Microfluidic synthesis of atto-liter scale double emulsions toward ultrafine hollow silica spheres with hierarchical pore networks. *Lab Chip* 12(24):5262–5271
- Jeong W-C, Lim J-M, Choi J-H, Kim J-H, Lee Y-J, Kim S-H, Lee G, Kim J-D, Yi G-R, Yang S-M (2012b) Controlled generation of submicron emulsion droplets via highly stable tip-streaming mode in microfluidic devices. *Lab Chip* 12(8):1446–1453
- Jiang S, Granick S (2007) Janus balance of amphiphilic colloidal particles. *J Chem Phys* 127:161102
- Kalman D, Wagner N (2009) Microstructure of shear-thickening concentrated suspensions determined by flow-USANS. *Rheol Acta* 48(8):897–908
- Kantak C, Zhu Q, Beyer S, Bansal T, Trau D (2012) Utilizing microfluidics to synthesize polyethylene glycol microbeads for Forster resonance energy transfer based glucose sensing. *Biomicrofluidics* 6(2):022006
- Kaufmann T, Gokmen MT, Rinnen S, Arlinghaus HF, Du Prez F, Ravoo BJ (2012) Bifunctional Janus beads made by “sandwich” microcontact printing using click chemistry. *J Mater Chem* 22(13):6190–6199
- Khan SA, Gunther A, Schmidt MA, Jensen KF (2004) Microfluidic synthesis of colloidal silica. *Langmuir* 20(20):8604–8611
- Kim S-H, Jeon S-J, Yi G-R, Heo C-J, Choi JH, Yang S-M (2008) Optofluidic assembly of colloidal photonic crystals with controlled sizes, shapes, and structures. *Adv Mater* 20(9):1649–1655
- Kim S-H, Shim JW, Lim J-M, Lee SY, Yang S-M (2009) Microfluidic fabrication of microparticles with structural complexity using photocurable emulsion droplets. *New J Phys* 11:075014
- Kim JH, Jeon TY, Choi TM, Shim TS, Kim S-H, Yang S-M (2013) Droplet microfluidics for producing functional microparticles. *Langmuir* (in press)
- Koh W-G, Pishko M (2003) Photoreaction injection molding of biomaterial microstructures. *Langmuir* 19(24):10310–10316
- Kohane DS (2007) Microparticles and nanoparticles for drug delivery. *Biotechnol Bioeng* 96(2):203–209
- Kuehne AJC, Weitz DA (2011) Highly monodisperse conjugated polymer particles synthesized with drop-based microfluidics. *Chem Commun* 47(45):12379–12381
- Kuijk A, van Blaaderen A, Imhof A (2011) Synthesis of monodisperse, rodlike silica colloids with tunable aspect ratio. *J Am Chem Soc* 133(8):2346–2349
- Kumacheva E, Garstecki P (2011) Microfluidic reactors for polymer particles. Wiley, Chichester
- Langer R, Peppas NA (2003) Advances in biomaterials, drug delivery, and bionanotechnology. *AIChE J* 49(12):2990–3006
- Lattuada M, Hatton TA (2011) Synthesis, properties and applications of Janus nanoparticles. *Nano Today* 6(3):286–308
- Lee Y, Wagner N (2003) Dynamic properties of shear thickening colloidal suspensions. *Rheol Acta* 42(3):199–208
- Lee JN, Park C, Whitesides GM (2003) Solvent compatibility of poly(dimethylsiloxane)-based microfluidic devices. *Anal Chem* 75:6544–6554
- Lee MH, Hribar KC, Brugarolas T, Kamat NP, Burdick JA, Lee D (2012) Harnessing interfacial phenomena to program the release properties of hollow microcapsules. *Adv Funct Mater* 22(1):131–138
- Li X, Cao HL, Gao S, Pan FY, Weng LQ, Song SH, Huang YD (2008) Preparation of body armour material of Kevlar fabric treated with colloidal silica nanocomposite. *Plast, Rubber Compos* 37(5–6):223–226
- Li W, Greener J, Voicu D, Kumacheva E (2009) Multiple modular microfluidic (M3) reactors for the synthesis of polymer particles. *Lab Chip* 9(18):2715–2721
- Lin R, Fisher JS, Simon MG, Lee AP (2012) Novel on-demand droplet generation for selective fluid sample extraction. *Biomicrofluidics* 6(2):024103
- Litvinov VM, Dias AA (2001) Analysis of network structure of UV-cured acrylates by ¹H NMR relaxation, ¹³C NMR spectroscopy, and dynamic mechanical experiments. *Macromolecules* 34(12):4051–4060
- Liu K, Deng Y, Zhang N, Li S, Ding H, Guo F, Liu W, Guo S, Zhao X-Z (2012) Generation of disk-like hydrogel beads for cell encapsulation and manipulation using a droplet-based microfluidic device. *Microfluid Nanofluid* 13(5):761–767

- Lu A-H, Salabas EL, Schüth F (2007) Magnetic nanoparticles: synthesis, protection, functionalization, and application. *Angew Chem Int Ed* 46(8):1222–1244
- Luo G, Du L, Wang Y, Lu Y, Xu J (2011) Controllable preparation of particles with microfluidics. *Particuology* 9(6):545–558
- Mark D, Haerberle S, Roth G, von Stetten F, Zengerle R (2010) Microfluidic lab-on-a-chip platforms: requirements, characteristics and applications. *Chem Soc Rev* 39(3):1153
- Marre S, Jensen KF (2010) Synthesis of micro and nanostructures in microfluidic systems. *Chem Soc Rev* 39(3):1183–1202
- Mazzitelli S, Capretto L, Carugo D, Zhang X, Piva R, Nastruzzi C (2011) Optimised production of multifunctional microfibrils by microfluidic chip technology for tissue engineering applications. *Lab Chip* 11(10):1776–1785
- McDonald JC, Whitesides GM (2002) Poly(dimethylsiloxane) as a material for fabricating microfluidic devices. *Acc Chem Res* 35(7):491–499
- Merkel TJ, Herlihy KP, Nunes J, Orgel RM, Rolland JP, DeSimone JM (2010) Scalable, shape-specific, top-down fabrication methods for the synthesis of engineered colloidal particles. *Langmuir* 26(16):13086–13096
- Merkel TJ, Chen K, Jones SW, Pandya AA, Tian S, Napier ME, Zamboni WE, DeSimone JM (2012) The effect of particle size on the biodistribution of low-modulus hydrogel PRINT particles. *J Control Release* 162(1):37–44
- Mitragotri S (2009) In drug delivery, shape does matter. *Pharm Res* 26(1):232–234
- Motomov M, Roiter Y, Tokarev I, Minko S (2010) Stimuli-responsive nanoparticles, nanogels and capsules for integrated multifunctional intelligent systems. *Prog Polym Sci* 35(1–2):174–211
- Mulligan M, Rothstein J (2012) Scale-up and control of droplet production in coupled microfluidic flow-focusing geometries. *Microfluid Nanofluid* 13(1):65–73
- Neethirajan S, Kobayashi I, Nakajima M, Wu D, Nandagopal S, Lin F (2011) Microfluidics for food, agriculture and biosystems industries. *Lab Chip* 11(9):1574–1586
- Negrete-Herrera N, Putaux J-L, Bourgeat-Lami E (2006) Synthesis of polymer/laponite nanocomposite latex particles via emulsion polymerization using silylated and cation-exchanged Laponite clay platelets. *Prog Solid State Chem* 34(2–4):121–137
- Nguyen KT, West JL (2002) Photopolymerizable hydrogels for tissue engineering applications. *Biomaterials* 23(22):4307–4314
- Nunes J, Herlihy KP, Mair L, Superfine R, DeSimone JM (2010) Multifunctional shape and size specific magneto-polymer composite particles. *Nano Lett* 10(4):1113–1119
- Panda P, Ali S, Lo E, Chung BG, Hatton TA, Khademhosseini A, Doyle PS (2008) Stop-flow lithography to generate cell-laden microgel particles. *Lab Chip* 8(7):1056–1061
- Park JI, Saffari A, Kumar S, Gunther A, Kumacheva E (2010) Microfluidic synthesis of polymer and inorganic particulate materials. *Annu Rev Mater Res* 40:415–443
- Pawar AB, Kretschmar I (2010) Fabrication, assembly, and application of patchy particles. *Macromol Rapid Commun* 31(2):150–168
- Pregibon DC, Toner M, Doyle PS (2006) Multifunctional encoded particles for high-throughput biomolecule analysis. *Science* 315(5817):1393–1396. doi:10.1126/science.1134929
- Qiang W, Wang Y, He P, Xu H, Gu H, Shi D (2008) Synthesis of asymmetric inorganic/polymer nanocomposite particles via localized substrate surface modification and miniemulsion polymerization. *Langmuir* 24(3):606–608
- Qin D, Xia Y, Whitesides GM (2010) Soft lithography for micro- and nanoscale patterning. *Nat Protoc* 5(3):491–502
- Raghavan SR, Khan SA (1997) Shear-thickening response of fumed silica suspensions under steady and oscillatory shear. *J Colloid Interface Sci* 185(1):57–67
- Rolland JP, Maynor BW, Euliss LE, Exner AE, Denison GM, DeSimone JM (2005) Direct fabrication and harvesting of monodisperse, shape-specific nanobiomaterials. *J Am Chem Soc* 127(28):10096–10100
- Rotem A, Abate AR, Utada AS, Van Steijn V, Weitz DA (2012) Drop formation in non-planar microfluidic devices. *Lab Chip* 12(21):4263–4268
- Santos-Martinez MJ, Prina-Mello A, Medina C, Radomski MW (2011) Analysis of platelet function: role of microfluidics and nanodevices. *Analyst* 136(24):5120–5126
- Seiffert S, Weitz DA (2010) Microfluidic fabrication of smart microgels from macromolecular precursors. *Polymer* 51(25):5883–5889
- Seiffert S, Romanowsky MB, Weitz DA (2010) Janus Microgels produced from functional precursor polymers. *Langmuir* 26(18):14842–14847
- Serra CA, Chang Z (2008) Microfluidic-assisted synthesis of polymer particles. *Chem Eng Technol* 31(8):1099–1115
- Shah RK, Shum HC, Rowat AC, Lee D, Agresti JJ, Utada AS, Chu L-Y, Kim J-W, Fernandez-Nieves A, Martinez CJ, Weitz DA (2008) Designer emulsions using microfluidics. *Mater Today* 11(4):18–27
- Shepherd RF, Conrad JC, Rhodes SK, Link DR, Marquez M, Weitz DA, Lewis JA (2006) Microfluidic assembly of homogeneous and Janus colloid-filled hydrogel granules. *Langmuir* 22(21):8618–8622
- Shepherd RF, Panda P, Bao Z, Sandhage KH, Hatton TA, Lewis JA, Doyle PS (2008) Stop-flow lithography of colloidal, glass, and silicon microcomponents. *Adv Mater* 20(24):4734–4739
- Shim TS, Kim S-H, Yang S-M (2013) Elaborate design strategies toward novel microcarriers for controlled encapsulation and release. *Part Part Syst Charact* 30(1):9–45
- Shum HC, Abate AR, Lee D, Studart AR, Wang B, Chen CH, Thiele J, Shah RK, Krummel A, Weitz DA (2010) Droplet microfluidics for fabrication of non-spherical particles. *Macromol Rapid Commun* 31(2):108–118
- Singh A, Sharma P, Garg V, Garg G (2010) Hydrogel: a review. *Int J Pharm Sci Rev Res* 4(2):016
- Solomon MJ, Zeitoun R, Ortiz D, Sung KE, Deng D, Shah A, Burns MA, Glotzer SC, Millunchick JM (2010) Toward assembly of non-close-packed colloidal structures from anisotropic pentamer particles. *Macromol Rapid Commun* 31(2):196–201
- Song Y, Modrow H, Henry LL, Saw CK, Doomes EE, Palshin V, Hormes J, Kumar CSSR (2006) Microfluidic synthesis of cobalt nanoparticles. *Chem Mater* 18(12):2817–2827
- Suh SK, Chapin SC, Hatton TA, Doyle PS (2012) Synthesis of magnetic hydrogel microparticles for bioassays and tweezer manipulation in microwells. *Microfluid Nanofluid* 13(4):665–674
- Tan J, Shah S, Thomas A, Ou-Yang HD, Liu Y (2012) The influence of size, shape and vessel geometry on nanoparticle distribution. *Microfluid Nanofluid* 14(1–2):1–11
- Tao AR, Habas S, Yang P (2008) Shape control of colloidal metal nanocrystals. *Small* 4(3):310–325
- Tao L, Hu W, Liu Y, Huang G, Sumer B, Gao J (2011) Shape-specific nanomedicine: emerging opportunities and challenges. *Exp Biol Med* 236:20–29
- Trietsch SJ, Hankemeier T, van der Linden HJ (2011) Lab-on-a-chip technologies for massive parallel data generation in the life sciences: a review. *Chemometr Intell Lab Syst* 108(1):64–75
- Utada AS, Chu LY, Fernandez-Nieves A, Link DR, Holtze C, Weitz DA (2007) Dripping, jetting, drops, and wetting: the magic of microfluidics. *MRS Bull* 32(09):702–708
- Wacker JB, Lignos I, Parashar VK, Gijs MAM (2012) Controlled synthesis of fluorescent silica nanoparticles inside microfluidic droplets. *Lab Chip* 12(17):3111–3116

- Wan J (2012) Microfluidic-based synthesis of hydrogel particles for cell microencapsulation and cell-based drug delivery. *Polymers* 4(2):1084–1108
- Wang J, Zhang J, Han J (2010) Synthesis of crystals and particles by crystallization and polymerization in droplet-based microfluidic devices. *Front Chem Eng China* 4(1):26–36
- Wassen S, Rondeau E, Sott K, Loren N, Fischer P, Hermansson A-M (2012) Microfluidic production of monodisperse biopolymer particles with reproducible morphology by kinetic control. *Food Hydrocoll* 28(1):20–27
- Weng SB, Kim IT, Qin D, Xia Y, Whitesides GM (1999) Formation of patterned microstructures of conducting polymers by soft lithography, and applications in microelectronic device fabrication. *Adv Mater* 11(12):1038–1041
- Wu Y, Joseph S, Aluru NR (2009) Effect of cross-linking on the diffusion of water, ions, and small molecules in hydrogels. *J Phys Chem B* 113(11):3512–3520
- Wurm F, Kilbinger AFM (2009) Polymeric Janus particles. *Angew Chem Int Ed* 48(45):8412–8421
- Xia Y, Rogers JA, Paul KE, Whitesides GM (1999) Unconventional methods for fabricating and patterning nanostructures. *Chem Rev* 99(7):1823–1848
- Xu S, Nie Z, Seo M, Lewis P, Kumacheva E, Stone HA, Garstecki P, Weibel DB, Gitlin I, Whitesides GM (2005) Generation of monodisperse particles by using microfluidics: control over size, shape, and composition. *Angew Chem Int Ed* 44(5):724–728
- Xuan X, Zhu J, Church C (2010) Particle focusing in microfluidic devices. *Microfluid Nanofluid* 9(1):1–16
- Yager P, Edwards T, Fu E, Helton K, Nelson K, Tam MR, Weigl BH (2006) Microfluidic diagnostic technologies for global public health. *Nature* 442(7101):412–418
- Yamagami T, Tanaka T, Suzuki T, Okubo M (2013) Preparation of hemispherical polymer particles via phase separation induced by micro-suspension polymerization. *Coll Polym Sci* 291(1):71–76
- Yang S-M, Kim S-H, Lim J-M, Yi G-R (2008) Synthesis and assembly of structured colloidal particles. *J Mater Chem* 18(19):2177–2190
- Yang S-Y, Cheng F-Y, Yeh C-S, Lee G-B (2010) Size-controlled synthesis of gold nanoparticles using a micro-mixing system. *Microfluid Nanofluid* 8(3):303–311
- Yang S, Guo F, Kiraly B, Mao X, Lu M, Leong KW, Huang TJ (2012) Microfluidic synthesis of multifunctional Janus particles for biomedical applications. *Lab Chip* 12(12):2097–2102
- Yin Y, Xia Y (2001) Self-assembly of monodispersed spherical colloids into complex aggregates with well-defined sizes, shapes, and structures. *Adv Mater* 13(4):267–271
- Yuet KP, Hwang DK, Haghgooie R, Doyle PS (2009) Multifunctional superparamagnetic Janus particles. *Langmuir* 26(6):4281–4287
- Zeng S, Liu X, Xie H, Lin B (2011) Basic technologies for droplet microfluidics. In: *Microfluidics*, vol 304. *Topics in Current Chemistry*. Springer, Berlin, pp 69–90
- Zhang Q, Lin B, Qin J (2012) Synthesis of shape-controlled particles based on synergistic effect of geometry confinement, double emulsion template, and polymerization quenching. *Microfluid Nanofluid* 12(1–4):33–39
- Zhao C-X, He L, Qiao SZ, Middelberg APJ (2011) Nanoparticle synthesis in microreactors. *Chem Eng Sci* 66(7):1463–1479